A tale of two tubeworms: taxonomy of vestimentiferans (Annelida: Siboglinidae) from the Mid-Cayman Spreading Centre

Magdalena N. Georgieva[1,2,†], Nadezhda N. Rimskaya-Korsakova[3†,*], Varvara I. Krolenko[3], Cindy Lee Van Dover[4], Diva J. Amon[5,6], Jonathan T. Copley[7], Sophie Plouviez[8], Bernard Ball[9], Helena Wiklund[1,10,11], Adrian G. Glover[1]

[1]Life Sciences Department, Natural History Museum, London, United Kingdom
[2]Univ. Brest, CNRS, Ifremer, UMR6197 Biologie et Ecologie des Ecosystèmes marins Profonds, Plouzané, France
[3]Department of Invertebrate Zoology, Faculty of Biology, Lomonosov Moscow State University, Moscow, Russia
[4]Division of Marine Science and Conservation, Nicholas School of the Environment, Duke University Marine Laboratory, Beaufort, North Carolina, USA
[5]SpeSeas, D'Abadie, Trinidad and Tobago
[6]Marine Science Institute, University of California, Santa Barbara, Santa Barbara, CA, USA
[7]Ocean & Earth Science, University of Southampton, Southampton, United Kingdom
[8]Department of Biology, University of Louisiana at Lafayette, Lafayette LA, USA
[9]School of Biology & Environmental Science, University College Dublin, Dublin, Ireland
[10]Department of Marine Sciences, University of Gothenburg, Gothenburg, Sweden
[11]Gothenburg Global Biodiversity Centre, Gothenburg, Sweden

[†]**these authors contributed equally to this work**
*__Correspondence:__ Nadezhda Rimskaya-Korsakova, nadezdarkorsakova@gmail.com

ORCIDs
Magdalena N. Georgieva, 0000-0002-1129-0571
Nadezda Rimskaya-Korsakova, 0000-0001-9576-2435
Varvara Krolenko, 0000-0002-9265-302X
Cindy Lee Van Dover, 0000-0001-9845-8391
Diva J. Amon, 0000-0003-3044-107X
Jonathan T. Copley, 0000-0003-3333-4325
Sophie Plouviez, 0000-0002-5211-9922
Bernard Ball, 0000-0002-9817-0993
Helena Wiklund, 0000-0002-8252-3504
Adrian G. Glover, 0000-0002-9489-074X

Running title: Two new species of vestimentiferans from the Mid-Cayman Spreading Centre

Abstract

The vestimentiferan tubeworm genera *Lamellibrachia* and *Escarpia* inhabit deep-sea chemosynthesis-based ecosystems, such as seeps, hydrothermal vents and organic falls, and have wide distributions across the Pacific, Atlantic and Indian Oceans. In 2010-2012 during initial explorations of hydrothermal vents of the Mid-Cayman Spreading Centre (MCSC), both genera were found to co-occur at the Von Damm Vent Field (VDVF), a site characterized by diffuse flow and thus resembling a 'hydrothermal seep'. Here, we erect two new vestimentiferan tubeworm species from the VDVF, ***Lamellibrachia judigobini*** sp. nov. and ***Escarpia tritentaculata*** sp. nov. *Lamellibrachia judigobini* sp. nov. differs genetically and morphologically from other *Lamellibrachia* species, and has a range that extends across the Gulf of Mexico, MCSC, off Trinidad and Tobago, and Barbados, as well as across both vents and seeps and 964 to 3304m water depth. *Escarpia tritentaculata* sp. nov. is distinguished from other *Escarpia* species primarily on morphology, and is known only from vents of the MCSC at 2300 m depth. This study highlights the incredible habitat flexibility of a single *Lamellibrachia* species and the genus *Escarpia*, as well as historic biogeographic connections to the eastern Pacific for *L. judigobini* sp. nov. and to the eastern Atlantic for *E. tritentaculata* sp. nov.

ZooBank: urn:lsid:zoobank.org:pub:D9F72BD4-FDE1-4C0A-B84B-A08D06F2A981

Keywords

Lamellibrachia, *Escarpia*, chemosynthesis, biodiversity, cold seep, Caribbean, plaque papillae, tentacles, pinnules, COI, 16S DNA, 18S DNA

Introduction

Annelids of the monophyletic lineage Vestimentifera (Siboglinidae; Caullery, 1914) are renowned for their colonisation and specialisation to life within deep-sea chemosynthetic environments, as well as the large sizes, rapid growth rate, and longevity of over 200 years that some species can achieve (Lutz *et al.* 1994; Bergquist *et al.* 2000; Southward *et al.* 2005; Durkin *et al.* 2017). The genera *Lamellibrachia* Webb, 1969 and *Escarpia* Jones, 1985 are considered basal to the vestimentiferan radiation (Li *et al.* 2015), and while certain vestimentiferan species are endemic to a particular chemosynthetic setting (e.g. *Riftia pachyptila* Jones, 1981 and *Ridgeia piscesae* Jones, 1985 are only found at hydrothermal vents), *Lamellibrachia* and *Escarpia* exhibit greater flexibility, occurring within deep-sea cold seeps (Gardiner and Hourdez 2003; Andersen *et al.* 2004; Miglietta *et al.* 2010), as well as at whale falls (Feldman *et al.* 1998), other organic falls (Hughes and Crawford 2008; Southward *et al.* 2011), and hydrothermal vents (Southward 1991; Plouviez *et al.* 2015). Such habitat flexibility is likely to have been key in enabling vestimentiferans to spread throughout the world's oceans.

First documented in 1969 (Webb 1969), *Lamellibrachia* comprises one of the most speciose vestimentiferan genera. Eight described *Lamellibrachia* species are known from tropical and temperate localities in both the Pacific and Atlantic Oceans (including the Mediterranean Sea) at depth ranges of 98-1800 m (McCowin and Rouse 2018). There are also a number of known but as yet undescribed *Lamellibrachia* species, known informally as *Lamellibrachia* sp. 1/cf. *luymesi*, *Lamellibrachia* sp. 2, *Lamellibrachia* sp. L4, *Lamellibrachia* sp. L5, *Lamellibrachia* sp. L6, and *Lamellibrachia* sp. Cauvery–Mannar Basin (Kojima *et al.* 2001; McCowin and Rouse 2018; McCowin *et al.* 2019; Mazumdar *et al.* 2021). Of these, *Lamellibrachia* sp. 1 and *Lamellibrachia* sp. 2 (described here and referred to hereafter as *Lamellibrachia judigobini* sp. nov.) occur in the Gulf of Mexico with several aspects of their biology and ecology already studied (Cordes *et al.* 2009; Miglietta *et al.* 2010; Thiel *et al.* 2012; Cowart *et al.* 2014). While *Lamellibrachia luymesi* van der Land & Nørrevang, 1975 has a similar geographic range as

that of *Lamellibrachia* sp. 1, *L. luymesi* generally inhabits depths of 400 to 800m, whereas *Lamellibrachia* sp. 1 occurs at 950 to 2320m and *L. judigobini* sp. nov. inhabits still deeper depths (1,175 to 2,320 m; Miglietta et al., 2010). *Lamellibrachia* sp. 1 is genetically very similar to *L. luymesi*, however *L. judigobini* sp. nov. is clearly a distinct species (Miglietta *et al.* 2010; Cowart *et al.* 2014). Genetic analyses have also confirmed that *L. judigobini* sp. nov. occurs at diffuse vents of the Mid-Cayman Spreading Centre (MCSC; also known as the Mid-Cayman Rise, MCR) at ~2300m depth (Plouviez *et al.* 2015; Plouviez *et al.* 2017), at the El Pilar seep site off Trinidad and Tobago between 1070m and 1629m depth (Amon *et al.* 2017), as well as at another seep site approximately 185km south-east of Barbados at ~1350m, known as Milano (Plouviez *et al.* 2017). At the MCSC, *L. judigobini* sp. nov. inhabits a sedimented, diffuse flow area of the off-axis Von Damm Vent Field (VDVF), characterised by low temperature fluids emanating from rock rubble (Connelly *et al.* 2012; Plouviez *et al.* 2015).

The genus *Escarpia* currently contains three species known from cold seeps and a whale fall off southern California/Mexico/Chile (*Escarpia spicata* Jones, 1985), seeps in the Gulf of Mexico (*Escarpia laminata* Jones, 1985), and seeps near the Congo River Canyon off the west coast of Africa (*Escarpia southwardae* Andersen *et al.*, 2004) (Jones 1985; Black *et al.* 1997; Feldman *et al.* 1998; Andersen *et al.* 2004; Cowart *et al.* 2013; Kobayashi and Araya 2018). Additionally, previously-undescribed *Escarpia* specimens have been reported from the MCSC, alongside *L. judigobini* sp. nov. (Plouviez *et al.* 2015), which we describe here as *Escarpia tritentaculata* sp. nov. An unknown *Escarpia* species has also been reported off the coast of southern Brazil at a pockmark field at ~1300m depth (Medina-Silva *et al.* 2018). Whilst *E. spicata*, *E. southwardae* and *E. laminata* demonstrate clear morphological differences, a range of molecular analyses conducted on the species have shown very few differences among them: they have intermixed COI, CYTB haplotypes, and microsatellites (Miglietta *et al.* 2010; Cowart *et al.* 2013), with the intron HbB2 being the only genetic marker that shows structure that reflects the geographic separation of the three species (Cowart *et al.* 2013). The southern-

Brazil *Escarpia* specimens also show little variation in COI to described *Escarpia* species (Medina-Silva *et al.* 2018).

In 2010, the remarkable and biologically-rich VDVF was discovered on the Mount Dent Oceanic Core Complex (OCC) seamount that rises about 2700m from the seafloor on the ultra-slow spreading MCSC (Connelly *et al.* 2012). The depth of the vent site is at 2300m and it is dominated at the actively venting areas by dense aggregations of alvinocarid shrimp, *Rimicaris hybisase* Nye, Copley, & Plouviez, 2012, alongside zoarcid fish, thorid shrimp, skeneid gastropods and squat lobsters (Plouviez *et al.*, 2015). On the flanks of the Mount Dent OCC, ~300m to the south of the main active venting region (~220°C), is an area characterised by weak diffuse flow (<31°C) named for a site marker (Marker X18) in Plouviez *et al.* (2015). It is a rubble-strewn region, with some low abundances of the alvinocarid shrimp and only slightly elevated temperatures. Amongst the rubble and boulders are populations of the two new tubeworm species described here, as well as *Bathymodiolus* mussels. The tubeworms and mussels are genetically close to known cold seep species from the Gulf of Mexico and Barbados, leading Plouviez *et al.* (2015) to describe the flank assemblage as a 'hydrothermal seep community' with intermediate chemical characteristics between vent and seep habitats. Critical to the long-term understanding of these unique vent/seep habitats is sound, integrative DNA taxonomy and with this in mind, we use in this study recent collections from the MCSC to formally describe *Lamellibrachia judigobini* sp. nov. and *Escarpia tritentaculata* sp. nov. and place these new taxa and records within an ecological, evolutionary and biogeographical context.

Materials and methods

Study area and sampling at sea

Samples analysed in the present study were collected on two voyages: RV *Atlantis* expedition AT18-16 (January 2012) and RRS *James Cook* expedition JC082 (February 2013), both to the

MCSC. Vestimentiferans were sampled from the 'Marker X18' region on the flanks of the Mount Dent OCC, VDVF (at approximately 18.375 N, 81.797 W, at 2360m depth; Fig. 1A, B; Table 1) by the manipulator arms of the *Jason-2* (January 2012) and *Isis* (February 2013) Remotely-Operated Vehicles (ROVs). Specimens were photographed *in-situ* prior to collection, and individual tubeworms were subsequently plucked from the boulder-strewn seafloor with the manipulator and placed in bioboxes on the front of the ROV. They were relatively easy to sample in this manner. Temperature measurements were taken with a probe in the area immediately around the animals while i*n-situ*. For the samples collected aboard JC082, samples were immediately placed into cold filtered seawater following the protocols in Glover *et al.* (2016) and then examined using microscopes and macro-photography equipment prior to preservation. Several tubes were recovered without animals inside, including one that had been subsequently colonised by capitellid worms, which have not yet been investigated. For *Lamellibrachia judigobini* sp. nov., four specimens each from JC082 and AT18-16 respectively were found with animals inside and used for the descriptive work (Table 1). Some dead tubes were also used for tube measurements. For *Escarpia tritentaculata* sp. nov., four specimens with animals were recovered from JC082 and four from AT18-16 (Table 1). Some specimens were dissected out of the tubes at sea before preservation for live specimen photography (Fig. 6). Photography was all done using a Panasonic Lumix G digital camera with 50mm macro lens mounted on a photography stand.

Samples were preserved aboard the research ships in either 80% non-denatured ethanol in DI water, or 10% formalin buffered in seawater, with fragments of each individual divided between the two preservation types. After preservation, specimens were photographed in the MSU using a Canon EOS 1D-X (Canon Inc., Tokyo, Japan) camera using Canon Lens 150 mm objective, while tubes at the NHM were additionally photographed with a Canon EOS 800D camera on a macrophotography stand. The tube photos were subsequently measured digitally using ImageJ software (Schneider *et al.* 2012).

176 *Morphological analyses*

177 A total of five specimens of worms and six tubes were used to describe MCSC *Lamellibrachia*
178 *judigobini* sp. nov., and six worms and 20 almost-complete tubes to describe MCSC *Escarpia*
179 *tritentaculata* sp. nov. (Supplementary Tables S1-S2).

180

181 For scanning electron microscopy (SEM), the structures of interest were postfixed with 1%
182 osmium tetroxide, dehydrated with increasing concentrations of ethanol and acetone, critical-
183 point dried and sputter coated with gold-palladium in order to study the morphology of the
184 animals' body surfaces, including cilia and plaque papillae. SEM studies were performed on
185 JEOL JSM-6380LA (JEOL Ltd., Tokyo, Japan) and Camscan-S2 (Cambridge Instruments).
186 Microscopes with accelerating voltage 20 kV and SEI mode (XXXX) at the Laboratory of
187 Electron Microscopy of Moscow State University, Russia.

188

189 The following morphological parameters were measured (Supplementary Tables S1-S2): tube
190 length, number of collars, tube diameter at the anterior opening and at the posterior part of
191 the tube, length and diameter of the obturacular region, number of branchial lamellae pairs
192 (in *Escarpia* and *Lamellibrachia*) and sheath lamellae pairs (*Lamellibrachia* only), thickness
193 of the cuticular crust and the length and width of the cuticular spines on the anterior frontal
194 surfaces of the obturacules (*Escarpia* only), diameters of the cuticular plaques of the papillae
195 in the vestimentum, the diameters of plaques in the anterior and posterior trunk, the ratio of
196 the obturaculum length to vestimentum length (*Lamellibrachia* only), length of the genital
197 grooves (if any), width of the ventral ciliary field, and length and diameter of the fragments of
198 the trunk. The shape and color of the tubes, the location of the tentacle pinnules, the state of
199 the posterior vestimental edge (fused or divided) were also noted. All studied samples were
200 incomplete and therefore the structure of opisthosomes could not be studied. To evaluate the
201 trends of the tubes, six complete tubes of *Lamellibrachia* and 20 complete tubes of *Escarpia*
202 were measured for maximum length and width, with data collected using ImageJ and plotted
203 in Microsoft Excel with linear regression.

DNA extraction, amplification and sequencing

Tissues from the body wall of four ethanol-preserved *Lamellibrachia judigobini* sp. nov. and three *Escarpia tritentaculata* sp. nov. individuals were cut for use in DNA extractions (Table 1). DNA was extracted using the Qiagen DNeasy Blood and Tissue Kit, following instructions provided by the manufacturer. Approximately 600-700 bp of COI, 440 bp of 16S, and 1600 bp of 18S were amplified for individuals of both species, while 650 bp of the HbB2 intron was also amplified for two *E. tritentaculata* sp. nov. individuals. Details of primers are listed in Supplementary Table S3. Polymerase chain reaction (PCR) mixtures contained 21 µl of Red Taq DNA Polymerase 1.1X MasterMix (VWR), 1 µl of each primer, and 2 µl of DNA template, giving a total volume of 25 µl for each reaction. PCR reactions were carried out in an Applied Biosystems Veriti thermocycler, using the following temperature profile for COI, 16S and 18S: 94°C/5 min, (94°C/45 s, 55°C/45s, 72°C/2 min)*35 cycles, 72°C/10 min; and the following temperature profile for HbB2 intron: 94°C/5 min, (94°C/1 min, 50°C/1.5 min, 72°C/2.5 min)*30 cycles, 72°C/7 min. PCR products were visualised on 1% agarose gels following electrophoresis, and subsequently sent to the Natural History Museum Sequencing Facility (UK) for purification and sequencing (in both forward and reverse directions) on an ABI 3730XL DNA Analyser (Applied Biosystems).

Molecular analyses

Newly generated COI, 16S and 18S sequences were aligned with existing sequences for vestimentiferans available on NCBI GenBank using Geneious v.10.2.5 (Kearse *et al.* 2012), making sure to include representatives of each known species, especially all *Lamellibrachia* and *Escarpia* species. Additional siboglinids as well as other annelid sequences were used as outgroups, resulting in a total of 36 terminal taxa (Supplementary Table S4). Phylogenetic analyses were conducted on a combined dataset of COI, 16S and 18S sequences in MrBayes v.3.2.6 (Ronquist *et al.* 2012), using JModelTest v.2.1.10 (Guindon and Gascuel 2003; Darriba *et al.* 2012) to select the best fitting model for each gene alignment according to the Akaike

information criterion. Under three substitution schemes, the maximum permissible in MrBayes, the best-fitting models were GTR+I+G for COI, GTR+G for 16S, and SYM+G 18S, and analyses were run three times for 10,000,000 generations using the above models. A maximum likelihood (ML) analysis was also performed on the same alignment in RAxML v.8.2.12 (Stamatakis 2014) under the GTR+G substitution model, with 1000 rounds of bootstrapping.

A COI alignment comprising only of *Lamellibrachia* species was used to calculate uncorrected pairwise distances, using PAUP* v.4.0a (build 165) (Swofford, 2002), with NCBI GenBank sequences outlined in Supplementary Table S4. This alignment was also inputted into the Automated Barcode Gap Discovery (ABGD) tool (Puillandre *et al.* 2012) to automatically detect species clusters within the genus. This was applied using both Jukes-Cantor and Kimura distances, and the following settings: pmin=0.001, pmax=0.1, Steps=20, X=1.5, Nb bins=30. An additional COI alignment that includes only *L. judigobini* sp. nov. individuals (Supplementary Table S5), as well as COI and HbB2 intron alignments including only *Escarpia* individuals (Supplementary Tables S6-S7), were also generated and used to draw haplotype networks in popART v.1.7 (Leigh and Bryant 2015) using TCS (Clement *et al.* 2002). Geographic occurrences of sequences reported to be from *L. judigobini* sp. nov. and *Escarpia* were also plotted to assess the ranges of the taxa (Fig. 1A).

Institutional abbreviations of deposited material are as follows: NHMUK, Natural History Museum UK; WSBS MSU, White Sea Branch of Zoological Museum of Moscow State University; UWI ZM, University of the West Indies Zoology Museum; PMJ Ann, Phyletic Museum Jena.

Results

Molecular species delimitation

The Bayesian phylogenetic analysis for the vestimentiferan lineage of Siboglinidae firstly confirms that, as previously reported (Plouviez *et al.* 2015), *Lamellibrachia judigobini* sp. nov. collected from the MCSC is conspecific with animals informally identified as *Lamellibrachia* 'sp. 2' (Fig. 2) known from a range of localities in the Gulf of Mexico and the Caribbean region (Fig. 1A; Supplementary Table S8). *L. judigobini* sp. nov. appears most closely related to *L. donwalshi* McCowin & Rouse, 2018 known from the Costa Rica Pacific margin, *L. luymesi* and *Lamellibrachia* sp. 1 also from the Gulf of Mexico and Caribbean, and *L. anaximandri* Southward *et al.*, 2011 from the Mediterranean (Fig. 2). The ML analysis did not provide evidence for a close relationship between *L. judigobini* sp. nov. and *L. donwalshi*, but did indicate good support for a clade containing *L. judigobini* sp. nov., *L. luymesi*, *Lamellibrachia* sp. 1, *L. donwalshi*, and *L. anaximandri*. (Fig. 2, *insert*).

Uncorrected COI pairwise genetic distances (Table 2) are a maximum of 0.7% between different *Lamellibrachia judigobini* sp. nov. populations, and range between 1.9-3.2% between *L. judigobini* sp. nov. and the most closely related *Lamellibrachia* species, with the 1.9% distance recorded between *L. judigobini* sp. nov. and *L. donwalshi*. Application of the ABGD tool, using both Jukes-Cantor and Kimura distances, showed identical results to the phylogeny, whereby all *L. judigobini* sp. nov. individuals were recovered as one species distinct from others in the genus (Supplementary Fig. S1; Group 9). A COI haplotype network for *L. judigobini* sp. nov. demonstrated that the majority of MCSC individuals share the same dominant haplotype as individuals from the Gulf of Mexico, El Pilar, and seeps off south-east Barbados (Fig. 3A).

Our phylogenetic analyses (Fig. 2) also confirmed the MCSC escarpiid to belong to the *Escarpia* species complex, which did not exhibit sufficient differences in the genes COI (Fig. 3), 16S and 18S on which to distinguish the MCSC population from known *Escarpia* species. Although COI was somewhat variable between *Escarpia* individuals, these differences did not

correspond to the different species (Fig. 3). MCSC individuals typed for the HbB2 intron demonstrated greatest similarity to *E. southwardae*, rather than the geographically closer *E. laminata* (Fig. 3).

Taxonomic accounts

Siboglinidae Caullery, 1914

Lamellibrachia Webb, 1969

Lamellibrachia judigobini sp. nov.

(Figs. 4A, E-G, 5A-C, 6A, 7, 8; Tables 3-4, Supplementary Table S1)

Lamellibrachia (Jollivet *et al.* 1990)

Lamellibrachia sp. (Olu *et al.* 1996)

Lamellibrachia sp. nov. (Nelson and Fisher 2000)

Lamellibrachia sp. (Cordes *et al.* 2007)

Lamellibrachia sp. 2 (Miglietta *et al.* 2010)

Lamellibrachia sp. 2 (Thiel *et al.* 2012)

Lamellibrachia sp. 2 (Jacobson *et al.* 2013)

Lamellibrachia sp. 2 (Cowart *et al.* 2014)

Lamellibrachia sp. 2 (Plouviez *et al.* 2015)

Lamellibrachia sp. 2 (Amon *et al.* 2017)

Type-locality: Caribbean Sea, Western Atlantic, Mid Cayman Spreading Centre, the Von Damm Vent Field, 'MarkerX18' site, 2362 meters depth, 18.37517 N, -81.79767 W.

Material examined. DNA: JC082 912 (holotype NHMUK XXX), JC082 913 (NHMUK XXX), JC082 920 (NHMUK XXX), JC082 925 (NHMUK XXX). Morphology: JC082 912 (holotype NHMUK XXX), AT18-16 MCR234 (paratype WSBS MSU ZMMU WS16820), AT 18-

16 MCR498 (paratype PMJ Ann 289), AT18-16 MCR667 (paratype UWIZM.2022.5), AT18-16 MCR691 (Tables 1, Supplementary Table S1).

Description. Tubes: those of six individuals nearly complete, although potentially missing posterior end, mean of 768 mm in length and ranging from maximum 1309mm to minimum 461mm (Figs. 4A, B, E-G, 5A-C, Supplementary Fig. S2). Maximum widths at the proximal points of tubes ranging from 10.1 mm to 16.3 mm, minimum width of tubes ~1mm at distal point. The holotype is 600 mm long, and 17 mm diameter anteriorly. Tubes generally straight in mid and anterior region, with pale cream-white, thick, hard wall although softer in mid-body region, anterior (100 mm) region of larger tubes characterised by fine overlaps of the outer layers, faintly collared or rough appearance, spaced 5-100mm apart (Figs. 5A-C), the tube becoming completely smooth in the mid-body region, finally tapering to a long, curling brown root of ~1mm in width, without obvious tube collars.

Obturaculum and tentacular crown: obturaculum is straight and narrow (Fig. 6A, 7A, Supplementary Table S1). Obturaculum length 9-16mm (n = 5; holotype 13mm); width 3.5-9mm in basis and 4-9mm (n = 5; in holotype 5-7mm), with bare anterior face, lacking any secreted structures (Fig. 6A). Lateral surface of obturaculum surrounded by tentacular plume. 3– 6 pairs sheath lamellae (n = 5, in holotype, 5 lamellae pairs; Figs 7B, C; 8A, 8a) enclose 11-23 pairs branchial lamellae (holotype 22-23 pairs; Figs 8B). The sheath lamellae consist of approximately full-length straight filaments without pinnules that are fused to each other. No medial sheath lamellae, only lateral ones. Often the number of left and right sheath pairs are not the same (Supplementary Table S1). Number of pairs of branchial lamellae can be different on the left and right sides, the difference between the lamellae could reach five, for example, 17 left pairs and 22 right pairs of branchial lamellae. Branchial filaments are also fused, but with free pinnulated tips (Fig. 8A). Pinnules are massive and tuberous (perhaps bumpiness is due to the fixation), located along the lateral side in a single row. Tentacles bear two rows of cilia: external and internal. Ratio of number of branchial lamellae pairs to obturaculum width varied from 1–3.3.

Vestimentum: is 16-25mm long (in holotype, 25mm) and 6-14mm wide (in holotype 10mm) with vestimental folds curled (Figs 7A-C, Supplementary Table S1). The collars of vestimental wings slightly overlapped the basal part of obturacular lobes. Collar has slight midventral separation and consisted of two lobes; left lobe covered by noticeably protruded right lobe (in holotype). Posterior ends of vestimental wings dissected, with drawn back rounded halves. Males have paired prominent dorsal genital grooves running along the vestimental cavity (Figs 8C, D). The genital ciliated grooves run along 4/5ths of the vestimentum length, with the 1/5th indent from the anteriomost vestimentum (in holotype, genital groove is 20mm long). Grooves flanked by ridge-like conspicuous epidermal folds. Ventral ciliary field is 1.5-3.5mm wide (in holotype, 3mm).

Trunk: the long trunk is noticeably tapered towards the posterior end (Fig. 6A). The anterior portion of the trunk is filled with the fragile dark trophosome tissue (Fig. 7D). The length of measured trunk fragments varied from 95+ to 130+mm (holotype more than 45mm), width from 1.5-6mm proximally to 0.5-9mm distally (holotype from 6-10mm).

Papillae: the papillae bear cuticular plaques on their tops (Figs. 8E-K, Supplementary Table S1). Vestimental papillae are abundant and spread regularly over the epidermis of the vestimentum (Figs. 8E, G). In the trunk, papillae are heterogeneously placed in the trunk: areas of condensed and loosely located papillae interchange (Figs. 8H-K). This change is apparent along the anterior-posterior axis, as well as in the dorsal-ventral axis and lateral axis. The vestimental papillae diameter varied from 54 to 104μm (in holotype, 74 to 97μm), the trunk papillae diameter varied from 55 to 140μm (in holotype, 98-140μm) anteriorly and 16 to 50μm (in holotype, 29-37μm) posteriorly. The anterior trunk papillae and vestimental papillae are dramatically protruded, with oval plaques having a thickened anterior margin in the shape of a crescent. The posterior trunk papillae almost do not protrude and are usually entirely retracted, with the level of the plaques lying at the level of the apical epidermis. Among the plaque papillae, there are many papillae bearing the opening of the tubiparous (pyriform) glands that secrete the tube material (Figs. 8E-H, J).

Opisthosome: not recovered.

Etymology. Named in honour of Caribbean marine ecologist, Dr Judith Gobin, Professor of Marine Biology at University of the West Indies, St. Augustine Campus, Trinidad and Tobago.

Distribution. The Caribbean region encompassing the Gulf of Mexico, MCSC, and the eastern Caribbean Sea off the islands of Trinidad and Tobago, and Barbados, at depths of 964 to 3304 m (Fig. 1A; Supplementary Table S8). Possibly also present at the Kick 'em Jenny submarine volcano off the island of Grenada and the Orenoque seep site off Venezuela (Table 4).

Remarks. Results of molecular analyses that include *Lamellibrachia judigobini* sp. nov. specimens from all four locations where this species has been recorded clearly differentiate it from other known *Lamellibrachia* species for which molecular data exists (Fig. 2; Table 2). The minimum pairwise uncorrected COI genetic distance of 1.9% between *L. judigobini* sp. nov. and other *Lamellibrachia* species is consistent with previous indications that lower values are not unusual for *Lamellibrachia* (McCowin and Rouse 2018), while the maximum COI genetic distance between *L. judigobini* sp. nov. specimens is more than a percent lower (Table 2). When compared with *L. victori* Mañé-Garzón & Montero, 1986 for which genetic data is unavailable, *L. judigobini* sp. nov. differs in most morphological features (Table 3).

The tubes of *L. judigobini* sp. nov. are, in all cases, likely incomplete with missing posterior roots, although in one single specimen a very long, brown root was present. The longest tube was measured at 1309mm, which is still shorter than the other largest species in the genus, *L. barhami* Webb, 1969 and *L. anaximandri* with tubes of 800-1546mm and 200-1530mm reported, respectively (Webb 1969; Southward 1991; Southward *et al.* 2011). The tubes from the VDVF appear to still be growing with no obvious reduction in growth in the larger specimens (Supplementary Fig. S2), however the sample size is quite small.

Lamellibrachia judigobini sp. nov. differs morphologically from other *Lamellibrachia* species in that it has the widest vestimental diameter, 6-14mm (n=5), one of the largest anterior tube apertures, 10.8-16.4mm (n=6), as well as the specific ranges of diameters of anterior trunk cuticular papillae plaque 55-140um (n=5) and posterior trunk cuticular papillae plaque 16-

50um (n=4) (Table 3). These values overlap with the ranges of the same parameters of other *Lamellibrachia* species, but do not match.

L. judigobini sp. nov. has ranges of lengths of tube, obturaculum, vestimentum, as well as the number of sheath lamellae, which are completely within the range of the East Atlantic *L. anaximandri* (Table 3). However, *L. anaximandri* has two rows of pinnules on the branchial filaments, whereas *L. judigobini* sp. nov. and other species such as *L. columna* Southward, 1991 have only one row on the dorsal, non-fused branchial tentacles. This character is potentially useful for distinguishing *Lamellibrachia* species, but currently the number of pinnule rows is reported for only three *Lamellibrachia* species.

In *L. judigobini* sp. nov., the whole range of number of sheath lamellae, 3-6 (n=5), and diameter of vestimentum cuticular papillae plaque, 54-104um, match the range of these characters of West Pacific *L. sagami* (accepted as *L. columna*) (Table 3). Moreover, the ranges of the obturaculum diameter and length, 3.5-9mm and 9-16mm (n=5), in *L. judigobini* sp. nov. falls within the range of values reported for *L. sagami* (Table 3).

L. judigobini sp. nov. and another West Atlantic species, *L. luymesi,* have the same obturaculum diameter range, 3.5-9mm (n=5) (Table 3). Also, the value range of the obturaculum length, 9-16mm (n=5), in *L. judigobini* sp. nov. falls within the range of these values of *L. luymesi*.

The range of values of number of branchial lamellae pairs, 11-23 (n = 5) in *L. judigobini* sp. nov. falls within that of East Pacific *L. donwalshi* (Table 3). However, the latter is distinguished by the smaller size of the tubes, the smallest size of vestimentum cuticular plaques, and the highest vestimentum/obturaculum ratio, 10, of the holotype.

The ranges of the obturaculum length, 9-16mm (n=5), in *L. judigobini* sp. nov. falls within the range of these values of one more East Pacific species *L. barhami* (Table 3).

Escarpia Jones, 1985

Escarpia tritentaculata sp. nov.

(Figs. 4A, C, D, 5D-H,6B, 9, 10, 11; Tables 6, Supplementary Table S2)

Type-locality: Caribbean Sea, Western Atlantic, Mid Cayman Spreading Centre, the Von Damm Vent Field, 'Marker X18' site, 2353m depth, 18.37480 N, -81.79738 W.

Material examined. DNA: JC082 915 (paratype WSBS MSU ZMMU WS16819), JC082 918 (NHMUK XXX), JC082 921 (NHMUK XXX). Morphology: JC082 915 (paratype WSBS MSU ZMMU WS16819), JC082 919 (holotype NHMUK XXX), AT18-16 MCR010 (paratype PMJ Ann 290), AT18-16 MCR017 (paratype PMJ Ann 291), AT18-16 MCR507, AT18-16 MCR1333 (Table 1). Tubes: JC082 904 (n=3), JC082-200 917 (n=4), JC082-200 916 (n=3), JC082-200 927 (n=3), JC082-200 934 (n=1), JC082-200 924 (n=7) (Supplementary Table S2).

Etymology. Named after the three types of filaments observed on the tentacular plume surrounding the obturacular lobes.

Description. Tubes: those of 20 individuals nearly complete, although potentially missing posterior end, mean of 334mm in length ranging from 192 mm to 480mm (Figs. 4C-D, 5D-H, Supplementary Fig. S3). Maximum width of tubes ranging from 4.2 to 11.5mm at the apical ends, minimum width of tubes ~0.6mm in posterior root region. Tubes generally straight at anterior 1/3-1/2 of length, posterior portion typically becoming strongly curved at mid-body and then heavily curling in the posterior region, colour white to faint green, slightly striped appearance in anterior region, especially green in mid-body region and becoming very smooth and faintly reflective in mid body, heavily curled and brown in the root (Figs. 5D-H). Anterior portion of tubes in some specimens with fine collars visible, completely smooth in others.

Obturaculum and tentacular crown: the obturacular lobes of six individuals are massive, short, and wide, 4 to 11mm in length (holotype 6mm), 5-10mm in diameter (holotype 9-10mm) (Figs. 6B, 9A-C, Supplementary Table S2). The ventral obturacular portions bear a prominent longitudinal ridge. The anterior surfaces of the obturacular lobes are covered by cuticular crust about 0.5-3mm thick (holotype 0.5mm). Among specimens, the crust colour ranges from dark brown to caramel. The crust has two layers: the upper columnar layer and the lower horizontal one (Fig. 10A). The latter one is composed of 3-32 horizontal layers (holotype three layers). Among the cuticular columns of the upper layer, two specimens of annelid Phyllodocidae sp.

were found (Fig. 9D, inset d). The anterior obturacular epidermis secretes a spike consisting of two halves, each spike half is secreted by each of the obturacular lobes (Fig. 9B-C). Often, spikes are not complete (perhaps because of predation). Spikes halves are 0.1-1 x 1-2.5mm in cross width x sagittal width (in holotype 0.5 x 2.5mm), covered by small spines. The tentacular plume surrounding the obturacular lobes is distinctly divided into three types of filaments: the external (close to collars), internal (close to obturaculum), and intermediate ones (Fig. 10B-F). The external filaments are thin, ca. 70μm in diameter, round in cross section (no longitudinal furrows), fused proximally for only 1/5 of their length, and bear two longitudinal rows of cilia, which extend along the whole length of a filament on external and internal surfaces (Fig. 10B-C). The internal filaments are thick, ca. 70-120μm in diameter, oval in cross section, bear two longitudinal furrows on the lateral surfaces, fused along almost their entire length, cilia are visible only at their bases (Fig. 10D, inset d). The intermediate filaments share features of both filaments: thick, ca. 70-120μm in diameter, oval in cross section, bearing two longitudinal furrows on the lateral surfaces, and bearing two longitudinal rows of cilia, which extend along external and internal surfaces of the filaments (Fig. 10F).

Vestimentum: the vestimentum is 10-16mm long (in holotype 15 mm) and 5-10mm wide (in holotype 10mm) (Supplementary Table S2). The basis of the obturacular lobes is slightly covered by the collar of the vestimental wings (Figs. 6B, 9A-C). The lateral vestimental wings run along the vestimentum; the posterior midventral margin of the wings is entire. The ventral ciliated field is 2-7mm wide (in holotype 7mm). Studied specimens are males, having genital grooves, 8-14mm long (in holotype 14 mm), in the vestimental cavities (Fig. 9B).

Trunk: the trunk fragments length varies from 11-110mm (in holotype 110+mm), diameter from 2-8mm (holotype 2-8mm). The represented small trunk fragments slightly taper posteriorly (Fig. 6B).

Plaque papillae: the papillae bear plaques; on the vestimental region they are topped by oval cuticular plaques from 48-108μm in diameter (in holotype, 53-78μm) (Figs. 11A-B, Supplementary Table S2). The plaques have a pronounced, thickened, and raised anterior margin compared with their posterior. Along both sides of the ventral ciliary field there is a

distinctive row of plaqued papillae (Fig. 11B, inset b). The trunk bears numerous distinct epidermal papillae topped with oval plaques from 61-164 μm in diameter (in holotype, 79-127μm) on the anterior trunk and from 45-106μm (in holotype 45-67μm) on the posterior trunk. There are papillae bearing plaques on the top the opening of the tubiparous (pyriform) glands.

Opisthosome: not recovered.

Distribution. Currently known only from the VDVF, MCSC, 2353-2376m depth.

Remarks. Genetic data for COI does not differentiate *Escarpia tritentaculata* sp. nov. from other species in the genus; this lack of separation of the currently described *Escarpia* species is well known, however new species have been erected despite this. Only the HbB2 intron separates currently described *Escarpia* species (Cowart *et al.* 2013), but MCSC specimens are identical to *E. southwardae* from near the Congo River Canyon off west Africa for this marker, rather than the geographically much closer species *E. laminata*. There remain several sound reasons to erect the new species *Escarpia tritentaculata* sp. nov.: 1) the genetic data suggests reasonable heterogeneity within the group, and separation based on the HbB2 intron yet is uncertain for COI, 2) whilst the MCSC specimens cannot be separated clearly based on DNA, the great distance between the MCSC and the Congo River Canyon is suggestive of isolation, perhaps in markers that we have not yet recovered and most importantly, 3) there are clear morphological differences between *E. tritentaculata* sp. nov. and all the currently described *Escarpia* species. In addition, the alternative would be to synonymise all known *Escarpia* species into a single taxon, which is likely to be incorrect based on our knowledge of genetic heterogeneity in the group and could cause an over-estimation of species ranges, which is not a conservative approach given the increasing anthropogenic threats to deep-sea habitats such as hydrothermal vents.

Escarpia tritentaculata sp. nov. differs morphologically from other *Escarpia* species (East Pacific *E. spicata*, West Atlantic *E. laminata*, and the East Atlantic *E. southwardae*) in having three types of plume filaments: external, internal, and intermediate (Table 5). The tentacles of the inner lamellae, which detach off from the tentacular plume, are fused only for 2/3 of their

lengths. They are thick and oval in the cross section. The tentacles of the external lamellae are free along their entire length. They are thin and round in the cross section. The tentacles of the intermediate lamellae are free as the external tentacles, and they are thick and oval like the internal tentacles.

E. tritentaculata sp. nov. has an obturaculum length of 4-11mm and width of 5-10mm, vestimentum length of 10-16mm and width of 5-10mm. These body proportion values of the new species are entirely encompassed by the range of these morphological characters of other species (Table 5). *E. tritentaculata* sp. nov. proportionally resembles the geographically close *E. laminata* in similar obturaculum width, vestimentum length and width. *E. tritentaculata* sp. nov. resembles the East Pacific species *E. spicata* in similar vestimentum diameter (5-10mm wide), and the spikes on the top of obturaculum are covered by spines in both species. But in contrast to *E. laminata* and *E. spicata,* the new species has plume filaments without pinnules, as observed in the eastern-Atlantic species *E. southwardae*. But *E. tritentaculata* sp. nov. differs from *E. southwardae* in that its internal and intermediate tentacles are oval in cross section, and not as flattened as in *E. southwardae* (Fig. 10D-F, Table 5).

The tubes of *E. tritentaculata* sp. nov. are likely incomplete in some cases, although the root region does seem to hold together more strongly than in the *Lamellibrachia* collected from the same site with the same method (plucking with the ROV manipulator from coarse gravel). The longest tube was measured at 481 mm which is considerably smaller than the maximum length reported for *E. southwardae* of 1860 mm (Andersen *et al.* 2004). The tubes appear to be still growing in the largest specimens, with no obvious reduction in growth rate observed (Supplementary Fig. S3). The anterior part of the tubes is straight and extends vertically, the posterior part instead forms tight loops, presumably used as anchors to the hard substrate. Other *Escarpia* species are reported to have straight tubes arising above the substrate (Jones 1985; Andersen *et al.* 2004; Kobayashi and Araya 2018).

Discussion

Biogeography of Lamellibrachia *species*

This study firstly provides an overdue taxonomic account for *Lamellibrachia judigobini* sp. nov., previously known as *Lamellibrachia* 'sp. 2' for at least 20 years (Table 4). This species has a wide Caribbean range, that based on genetic analyses, includes the northern Gulf of Mexico, the MCSC, as well as seeps 185 km south-east of Barbados and the El Pilar seeps off Trinidad and Tobago (Fig. 1A), throughout which genetic connectivity appears to be maintained (Fig. 3). In addition, this species possibly also occurs at Grenada's Kick 'em Jenny submarine volcano (2000m depth; Carey et al., 2014, 2015), and the Venezuelan Orenoque seeps located approximately 115km south-east of El Pilar (1700-2000 m depth) (Jollivet *et al.* 1990; Cordes *et al.* 2007), but these records are as yet unconfirmed. Morphologically, the MCSC *L. judigobini* sp. nov. specimens most closely resemble species from the Mediterranean Sea and west part of the Pacific Ocean (*L. anaximandri, L. sagami*) than species inhabiting the Gulf of Mexico (*L. luymesi*) or eastern part of the Pacific Ocean (*L. barhami*) (Table 3). However, genetic data support a close relationship between *L. judigobini* sp. nov. and Gulf of Mexico (*L. luymesi*, *Lamellibrachia* sp. 1) and Mediterranean *Lamellibrachia* species (*L. anaximandri*), as well as *L. donwalshi* from the Pacific margin of Costa Rica (Fig. 2). The results of our Bayesian phylogenetic analysis are also consistent with the results of Southward *et al.* (2011) and McCowin & Rouse (2018) in which Pacific *Lamellibrachia* species appear more basal in phylogenetic analyses (Fig. 2), indicating that *Lamellibrachia* likely originated in the Pacific and subsequently colonised the Atlantic. The high COI similarity between *L. judigobini* sp. nov. (964 to 3304m depth) and *L. donwalshi*, which occurs at around 1000 m depth, supports the occurrence of a vicariant event that possibly separated these two species after the closing of the isthmus of Panama as suggested by McCowin & Rouse (2018), which started to form ~9-12 million years ago (O'Dea *et al.* 2016). Depth appears to be the most likely cause for differentiation between *L. judigobini* sp. nov. and *L. luymesi*, but the overlap in depth range between *L. judigobini* sp. nov. and *Lamellibrachia* sp. 1 from the Gulf of Mexico suggests there may also be other important environmental factors (Miglietta *et al.* 2010).

Biogeography of Escarpia *species*

Consistent with previous descriptions of *Escarpia* species and evidence based on microsatellites (Cowart *et al.* 2013), we erect *Escarpia tritentaculata* sp. nov. on the basis of specimens examined from the MCSC, due to clear morphological differences such as the presence of three types of plume filaments. *E. tritentaculata* sp. nov. occurs geographically closest to the Gulf of Mexico species *E. laminata*, and it is possible that *E. tritentaculata* sp. nov. may also occur at the Orenoque seeps, from which *Escarpia* specimens are reported as *Escarpia* cf. *laminata* (Olu *et al.* 1996). The similar seep environments that these species inhabit and evolved within could have resulted in *E. tritentaculata* sp. nov. and *E. laminata* demonstrating analogous genetic markers and morphological characters (such as comparable proportions of obturaculum and vestimentum). But in this case, species differentiation does not appear as a result of depth preferences as *E. laminata* occurs at depths of 2200 to 3300m (McMullin *et al.* 2003), which overlaps with the recorded depth of ~2500m for *E. tritentaculata*. At the same time, our genetic (HbB2 intron) and morphological data (absence of pinnules) hints at a connection between *E. tritentaculata* sp. nov. and *E. southwardae* described from the Congo River Canyon off west Africa (Fig. 3). However, active trans-Atlantic connectivity between these two sites is unlikely given the great distance (at least 6,800km) between the MCSC and the Congo River Canyon, and the observed lack of trans-Atlantic connectivity for other vestimentiferan species such as those in the genus *Lamellibrachia* (McCowin and Rouse 2018). And finally, our genetic and morphological data (presence of spike spines) also suggest that *E. tritentaculata* sp. nov. and East Pacific *E. spicata* are closely related, but these species are separated due to closure of the strait at the site of Mesoamerica (Karaseva *et al.* 2016).

Connectivity across chemosynthetic habitats in the Atlantic

Rather than contemporary gene flow, the observed genetic similarity between *Lamellibrachia judigobini* sp. nov. and *L. anaximandri*, as well as between *Escarpia tritentaculata* sp. nov. and *E. southwardae*, hints at potential historic connectivity across chemosynthetic habitats in

593 the Atlantic. Other species present at the MCSC, notably the abundant vent shrimp species
594 *Rimicaris hybisae*, demonstrate phylogenetic connections to the Mid-Atlantic Ridge as the
595 closest known relative of *R. hybisae* is the Mid-Atlantic Ridge species *R. chacei* (Plouviez *et*
596 *al.* 2015; Vereshchaka *et al.* 2015). Our analyses expand such Atlantic connections across the
597 entire Atlantic basin. Basin-scale distributions for other chemosynthetic taxa, possibly
598 through stepping-stone dispersal, have also been reported for the siboglinid species
599 *Sclerolinum contortum*, which is known from vents in the Southern Ocean as well as Arctic
600 vents and seeps (Georgieva *et al.* 2015; Eilertsen *et al.* 2018). This 'weedy' species can also
601 colonise a range of chemosynthetic habitats, and supports the idea that taxa with broad habitat
602 preferences (e.g. both 'hydrothermal seeps' and cold seeps) have the ability to spread at ocean-
603 basin scales.
604
605 *Unusual growth habit of* L. judigobini *sp. nov.*
606 At the MCSC, *Lamellibrachia judigobini* sp. nov. and *Escarpia tritentaculata* sp. nov. occupy
607 diffuse flow vent habitat at the VDVF that is more characteristic of a seep, due to the low
608 temperatures of fluids (~31°C) and the high concentrations of both hydrogen sulfide (3.2 to
609 5.3 mM) and methane (2.8 to 3.1 mM) (Connelly *et al.* 2012; Reveillaud *et al.* 2016). The
610 parallel-to-seafloor and generally unidirectional growth habit of the tubes of *L. judigobini* sp.
611 nov. is notable (Fig. 4A) and is mirrored by tubeworms presumed to be conspecifics at the El
612 Pilar seeps (Fig. 4G). The anterior surfaces of *E. southwardae* tubes are inhabited by
613 symbionts that reduce sulfate to hydrogen sulfide, which in turn is used by the host's
614 endosymbionts as an energy source for carbon fixation and growth of the holobiont (Duperron
615 *et al.* 2014). Seep fauna at VDVF also obtain energy from hydrogen sulfide produced by
616 microbial reduction of sulfate (Bennett *et al.* 2015). The microbial sulfate reduction and
617 overall high hydrogen sulfide content in the VDVF could account for the unique growth habit
618 of *L. judigobini* sp. nov., whereby the anterior end remains within a zone where hydrogen
619 sulfide is available. Alternatively, the parallel-to-seafloor growth of the tubes could occur due
620 to a combination of weak fluid flow and strong mixing. Indeed, it was noted during collection

621 that tubes are easily dislodged from the rubbly sediment at VDVF, making dislodgement more
622 likely if the tubes were to grow erect.
623
624 *Remarks on the association with additional fauna*
625 At the VDVF site of the MCSC where *Lamellibrachia judigobini* sp. nov. and *Escarpia*
626 *tritentaculata* sp. nov. occurred together, these species were associated with additional fauna
627 in areas of diffuse flow. Numerous *Iheyaspira bathycodon* Nye, Copley, Linse & Plouviez,
628 2013 gastropods and occasional *Lebbeus virentova* Nye, Copley, Plouviez & Van Dover, 2013
629 shrimps were seen around the tubeworms, likely exploiting the same fluid sources for
630 nutrition and possibly benefitting from habitat structure provided by the rubbly sediment and
631 *L. judigobini* sp. nov. and *E. tritentaculata* sp. nov. tubes (Fig. 4B). Additionally, during the
632 JC082 collections, a large capitellid annelid was observed occupying an empty *L. judigobini*
633 sp. nov. tube, demonstrating that the tubes of these vestimentiferans can still serve to provide
634 habitat after the death of the worms.
635
636 Bivalves were surprisingly sparse at VDVF (Plouviez *et al.* 2015), but the mussel species
637 *Bathymodiolus boomerang* Cosel & Olu, 1998 was dominant at the El Pilar seeps off Trinidad
638 and Tobago that form part of the range of *L. judigobini* sp. nov. At El Pilar, *L. judigobini* sp.
639 nov. occupied the ecotone between mussel beds and authigenic carbonates hosting non-
640 chemosynthetic fauna (Amon *et al.* 2017) as they are able to exploit sulfide deeper in the
641 sediment at less active locations through their extensive posterior tube regions (Freytag *et al.*
642 2001), while the mussel relies on drawing near-bottom water into its mantle cavity through its
643 gill cilia. Shrimp (*Alvinocaris* cf. *muricola* Williams, 1998) and gastropods (*Kanoia* cf.
644 *meroglypta* J. H. McLean & Quinn, 1987) were often associated with *L. judigobini* sp. nov. at
645 El Pilar (Fig. 4E, G), albeit different species to those at VDVF, which were again likely clustered
646 around tubes to benefit from higher productivity around seep fluid outlets. In addition,
647 *Neovermilia* sp. serpulid tubeworms and extensive microbial mats in some sedimented areas
648 were visually dominant at El Pilar, with microbial mats also occasionally covering *L.*

649 *judigobini* sp. nov. tubes (Fig. 4G). This fowling of *L. judigobini* sp. nov. tubes may also reflect
650 microenvironmental conditions whereby the recumbent anterior ends of *L. judigobini* sp. nov.
651 tubes are positioned in optimal conditions for microbial growth. The lack of observed co-
652 occurrence of other vent and seep fauna at the VDVF and El Pilar sites occupied by *L.*
653 *judigobini* sp. nov. again highlights the flexible habitat preferences and wide distribution of
654 this species in the region.
655
656 **Conclusion**
657
658 We have described two new species from a unique and hitherto poorly-studied hydrothermal
659 vent in the Caribbean region, the discovery of which in 2010 was a major surprise as it was
660 previously not expected that ultra-slow spreading ridges could support such active
661 hydrothermalism. The presence of these typically seep-dwelling taxa on a hydrothermal vent,
662 albeit with fairly low temperature flow, greatly increases our understanding of the role of a
663 range of chemosynthetic habitats in driving evolution and adaptive radiation in the deep sea.
664 It is likely that these are relatively weedy chemosynthetic species that are able to colonise a
665 range of habitats, as exemplified by their presence also in the Gulf of Mexico and other
666 Caribbean seep sites. Taxonomic works, undertaken using integrative DNA taxonomy are
667 critical to the long-term iterative building of biogeographic knowledge in these unique and
668 potentially-threatened habitats.
669
670 **Acknowledgements**
671
672 We thank the captain, crew, and ROV teams of the RV Atlantis AT18-16 (January 2012) and
673 RRS James Cook JC082 (February 2013) expeditions. We are grateful to Ann Andersen for
674 unique data on the morphometry of *E. southwardae* and fruitful help in the comparative
675 analysis of *Escarpia* species, and to Tim Le Bas for producing the bathymetric map of the
676 VDVF.

Declaration of funding

MG and AG were partly supported by the United Kingdom Natural Environment Research Council (grant to AG, number NE/R000670/1). Research cruise JC082 was funded by UK NERC grant NE/F017774/1 to JTC. MG is also grateful for support from an Ifremer postdoctoral fellowship. NNRK was supported by the Russian Science Foundation, project № 20-74-10011. The work was performed at the User Facilities Center of Lomonosov Moscow State University with financial support of the Ministry of Education and the Science of Russian Federation, No. 121032300121-0. CLVD, SP, and BB were supported by the US National Science Foundation (NSF, Biological Oceanography) award OCE-1031050 to CLVD and by Duke University.

Data availability

The raw data are available in Supplementary Tables S1-S8 and Supplementary Figures S2-S3.

Conflicts of interest

The authors declare that they have no competing interests.

References

Amon DJ, Gobin J, Van Dover CL, Levin LA, Marsh L, Raineault NA (2017). Characterization of methane-seep communities in a deep-sea area designated for oil and natural gas exploitation off Trinidad and Tobago. *Frontiers in Marine Science* **4**, 342. doi:10.3389/fmars.2017.00342

Andersen AC, Hourdez S, Marie B, Jollivet D, Lallier FH, Sibuet M (2004). *Escarpia southwardae* sp. nov., a new species of vestimentiferan tubeworm (Annelida, Siboglinidae) from West African cold seeps. *Canadian Journal of Zoology* **82**, 980–999. doi:10.1139/z04-049

Bennett SA, Dover C Van, Breier JA, Coleman M (2015). Effect of depth and vent fluid composition on the carbon sources at two neighboring deep-sea hydrothermal vent

706 fields (Mid-Cayman Rise). *Deep Sea Research Part I: Oceanographic Research Papers*
707 **104**, 122–133. doi:10.1016/j.dsr.2015.06.005
708 Bergquist DC, Williams FM, Fisher CR (2000). Longevity record for deep-sea invertebrate.
709 *Nature* **403**, 499–500. doi:10.1038/35000647
710 Black MB, Halanych KM, Maas PAY, Hoeh WR, Hashimoto J, Desbruyeres D, Lutz RA,
711 Vrijenhoek RC (1997). Molecular systematics of vestimentiferan tubeworms from
712 hydrothermal vents and cold-water seeps. *Marine Biology* **130**, 141–149.
713 Carey S, Ballard R, Bell KLC, Bell RJ, Connally P, Dondin F, Fuller S, Gobin J, Miloslavich P,
714 Phillips B, Roman C, Seibel B, Siu N, Smart C (2014). Cold seeps associated with a
715 submarine debris avalanche deposit at Kick'em Jenny volcano, Grenada (Lesser
716 Antilles). *Deep Sea Research Part I: Oceanographic Research Papers* **93**, 156–160.
717 doi:10.1016/j.dsr.2014.08.002
718 Carey S, Bell KLC, Roman C, Dondin F, Robertson R, Gobin J, Wankel S, Michel APM, Amon
719 D, Marsh L, Smart C, Vaughn I, Ball B, Rodrigue K, Haldeman M, George A, Ballard RD
720 (2015). Exploring Kick'em Jenny submarine volcano and the Barbados cold seep
721 province, Southern Lesser Antilles. *Oceanography* **28**, 38–39.
722 doi:10.5670/oceanog.2015.supplement.01
723 Caullery M (1914). Sur les Siboglinidae, type nouveau d'invertébrés receuillis par l'expédition
724 du Siboga. *Comptes Rendus Hebdomadaires des Séances de l'Académie des Sciences*
725 **158**, 2014–2017.
726 Clement M, Snell Q, Walke P, Posada D, Crandall K (2002). TCS: estimating gene
727 genealogies. In 'Proceedings of the 16th International Parallel and Distributed
728 Processing Symposium'. pp. 2:184
729 Connelly DP, Copley JT, Murton BJ, Stansfield K, Tyler PA, German CR, Van Dover CL,
730 Amon D, Furlong M, Grindlay N, Hayman N, Hühnerbach V, Judge M, Le Bas T,
731 McPhail S, Meier A, Nakamura K, Nye V, Pebody M, Pedersen RB, Plouviez S, Sands C,
732 Searle RC, Stevenson P, Taws S, Wilcox S (2012). Hydrothermal vent fields and
733 chemosynthetic biota on the world's deepest seafloor spreading centre. *Nature*

Communications **3**, 620. doi:10.1038/ncomms1636

Cordes EE, Bergquist DC, Fisher RC (2009). Macro-ecology of Gulf of Mexico cold seeps. *Annual Review of Marine Science* **1**, 143–168.

Cordes EE, Carney SL, Hourdez S, Carney RS, Brooks JM, Fisher CR (2007). Cold seeps of the deep Gulf of Mexico: community structure and biogeographic comparisons to Atlantic equatorial belt seep communities. *Deep Sea Research I* **54**, 637–653.

von Cosel R, Olu K (1998). Gigantism in Mytilidae: a new *Bathymodiolus* from cold seeps on the Barbados accretionary prism. *Comptes-Rendus de l'Académie des Sciences, ser. 3, Sciences de la Vie* **321**, 655–663.

Cowart DA, Halanych KM, Schaeffer SW, Fisher CR (2014). Depth-dependent gene flow in Gulf of Mexico cold seep *Lamellibrachia* tubeworms (Annelida, Siboglinidae). *Hydrobiologia* **736**, 139–154. doi:10.1007/s10750-014-1900-y

Cowart DA, Huang C, Arnaud-Haond S, Carney SL, Fisher CR, Schaeffer SW (2013). Restriction to large-scale gene flow vs. regional panmixia among cold seep *Escarpia* spp. (Polychaeta, Siboglinidae). *Molecular Ecology* **22**, 4147–4162. doi:10.1111/mec.12379

Darriba D, Taboada GL, Doallo R, Posada D (2012). jModelTest 2: more models, new heuristics and parallel computing. *Nature Methods* **9**, 772.

Duperron S, Gaudron SM, Lemaitre N, Bayon G (2014). A microbiological and biogeochemical investigation of the cold seep tubeworm *Escarpia southwardae* (Annelida: Siboglinidae): Symbiosis and trace element composition of the tube. *Deep Sea Research Part I: Oceanographic Research Papers* **90**, 105–114. doi:10.1016/j.dsr.2014.05.006

Durkin A, Fisher CR, Cordes EE (2017). Extreme longevity in a deep-sea vestimentiferan tubeworm and its implications for the evolution of life history strategies. *The Science of Nature* **104**, 63. doi:10.1007/s00114-017-1479-z

Eilertsen MH, Georgieva MN, Kongsrud JA, Linse K, Wiklund H, Glover AG, Rapp HT (2018). Genetic connectivity from the Arctic to the Antarctic: *Sclerolinum contortum*

762 and *Nicomache lokii* (Annelida) are both widespread in reducing environments.
763 *Scientific Reports* **8**, 4810. doi:10.1038/s41598-018-23076-0
764 Feldman R, Shank T, Black M, Baco A, Smith C, Vrijenhoek R (1998). Vestimentiferan on a
765 whale fall. *Biological Bulletin* **194**, 116–119.
766 Freytag JK, Girguis PR, Bergquist DC, Andras JP, Childress JJ, Fisher CR (2001). A paradox
767 resolved: sulfide acquisition by roots of seep tubeworms sustains net chemoautotrophy.
768 *Proceedings of the National Academy of Sciences of the United States of America* **98**,
769 13408–13413. doi:10.1073/pnas.231589498
770 Gardiner SL, Hourdez S (2003). On the occurrence of the vestimentiferan tube worm
771 *Lamellibrachia luymesi* van der Land and Nørrevang, 1975 (Annelida: Pogonophora) in
772 hydrocarbon seep communities in the Gulf of Mexico. *Proceedings of the Biological*
773 *Society of Washington* **116**, 380–394.
774 Georgieva MN, Wiklund H, Bell JB, Eilertsen MH, Mills RA, Little CTS, Glover AG (2015). A
775 chemosynthetic weed: the tubeworm *Sclerolinum contortum* is a bipolar, cosmopolitan
776 species. *BMC Evolutionary Biology* **15**, 280. doi:10.1186/s12862-015-0559-y
777 Glover AG, Dahlgren T, Wiklund H, Mohrbeck I, Smith C (2016). An end-to-end DNA
778 taxonomy methodology for benthic biodiversity survey in the Clarion-Clipperton Zone,
779 central Pacific abyss. *Journal of Marine Science and Engineering* **4**, 2.
780 doi:10.3390/jmse4010002
781 Guindon S, Gascuel O (2003). A simple, fast and accurate method to estimate large
782 phylogenies by maximum-likelihood. *Systematic Biology* **52**, 696–704.
783 Gustafson RG, Turner RD, Lutz RA, Vrijenhoek RC (1998). A new genus and five new species
784 of mussels (Bivalvia: Mytilidae) from deep-sea sulfide/hydrocarbon seeps in the Gulf of
785 Mexico. *Malacologia* **40**, 63–112.
786 Hughes DJ, Crawford M (2008). A new record of the vestimentiferan *Lamellibrachia* sp.
787 (Polychaeta: Siboglinidae) from a deep shipwreck in the eastern Mediterranean. *Marine*
788 *Biodiversity Records* **1**, e21. doi:10.1017/S1755267206001989
789 Jacobson A, Plouviez S, Thaler AD, Van Dover CL (2013). Characterization of 9 polymorphic

790 microsatellite loci in *Lamellibrachia* sp. 2, a tubeworm found at deep-sea hydrothermal
791 vents and cold seeps. *Conservation Genetics Resources* **5**, 1005–1007.
792 doi:10.1007/s12686-013-9955-z
793 Jollivet D, Faugeres J-C, Griboulard R, Desbruyers D, Blanc G (1990). Composition and
794 spatial organization of a cold seep community on the South Barbados accretionary
795 prism: Tectonic, geochemical and sedimentary context. *Progress in Oceanography* **24**,
796 25–45. doi:10.1016/0079-6611(90)90017-V
797 Jones ML (1985). On the Vestimentifera, new phylum: six new species, and other taxa, from
798 hydrothermal vents and elsewhere. *Bulletin of the Biological Society of Washington* **6**,
799 117–158.
800 Jones ML (1981). *Riftia pachyptila*, new genus, new species, the vestimentiferan worm from
801 the Galápagos Rift geothermal vents. *Proceedings of the Biological Society of*
802 *Washington* **93**, 1295–1313.
803 Karaseva NP, Rimskaya-Korsakova NN, Galkin S V., Malakhov V V. (2016). Taxonomy,
804 geographical and bathymetric distribution of vestimentiferan tubeworms (Annelida,
805 Siboglinidae). *Biology Bulletin* **43**, 937–969. doi:10.1134/S1062359016090132
806 Kearse M, Moir R, Wilson A, Stones-Havas S, Cheung M, Sturrock S, Buxton S, Cooper A,
807 Markowitz S, Duran C, Thierer T, Ashton B, Meintjes P, Drummond A (2012). Geneious
808 Basic: an integrated and extendable desktop software platform for the organization and
809 analysis of sequence data. *Bioinformatics* **28**, 1647–1649.
810 doi:10.1093/bioinformatics/bts199
811 Kobayashi G, Araya JF (2018). Southernmost records of *Escarpia spicata* and
812 *Lamellibrachia barhami* (Annelida: Siboglinidae) confirmed with DNA obtained from
813 dried tubes collected from undiscovered reducing environments in northern Chile Ed F
814 ZHANG. *PLoS ONE* **13**, e0204959. doi:10.1371/journal.pone.0204959
815 Kobayashi G, Miura T, Kojima S (2015). *Lamellibrachia sagami* sp. nov., a new
816 vestimentiferan tubeworm (Annelida: Siboglinidae) from Sagami Bay and several sites
817 in the northwestern Pacific Ocean. *Zootaxa* **4018**, 97. doi:10.11646/zootaxa.4018.1.5

Kojima S, Ohta S, Yamamoto T, Miura T, Fujiwara Y, Hashimoto J (2001). Molecular taxonomy of vestimentiferans of the western Pacific and their phylogenetic relationship to species of the eastern Pacific. I. Family Lamellibrachiidae. *Marine Biology* **139**, 211–219. doi:10.1007/s002270100581

van der Land J, Nørrevang A (1977). Structure and relationships of *Lamellibrachia* (Annelida, Vestimentifera). *Det Kongelige Danske Videnskabernes Selskab Biologiske Skrifter* **21**, 1–102.

van der Land J, Nørrevang A (1975). The systematic position of *Lamellibrachia* (Annelida, Vestimentifera). *Zeitschrift für zoologische Systematik und Evolutionsforschung Sonderheft* **[1975]**, 86–101.

Leigh JW, Bryant D (2015). popart: full-feature software for haplotype network construction Ed S Nakagawa. *Methods in Ecology and Evolution* **6**, 1110–1116. doi:10.1111/2041-210X.12410

Li Y, Kocot KM, Schander C, Santos SR, Thornhill DJ, Halanych KM (2015). Mitogenomics reveals phylogeny and repeated motifs in control regions of the deep-sea family Siboglinidae (Annelida). *Molecular phylogenetics and evolution* **85**, 221–229. doi:10.1016/j.ympev.2015.02.008

Lutz RA, Shank TM, Fornari DJ, Haymon RM, Lilley MD, Von Damm KL, Desbruyeres D (1994). Rapid growth at deep-sea vents. *Nature* **371**, 663–664. doi:10.1038/371663a0

Mañé-Garzón F, Montero R (1986). Sobre una nueva forma de verme tubícola *Lamellibrachia victori* n. sp. (Vestimentifera) proposicion de un nuevo phylum: Mesoneurophora. *Revista de Biologia de Uruguay* **8**, 1–28.

Mazumdar A, Dewangan P, Peketi A, Badesaab F, Sadique M, Sivan K, Mathai J, Ghosh A, Zatale A, Pillutla SPK, Uma C, Mishra CK, Fernandes W, Tyagi A, Paul T (2021). The first record of the genus *Lamellibrachia* (Siboglinidae) tubeworm along with associated organisms in a chemosynthetic ecosystem from the Indian Ocean: A report from the Cauvery–Mannar Basin. *Journal of Earth System Science* **130**, 94. doi:10.1007/s12040-021-01587-1

McCowin MF, Rouse GW (2018). A new *Lamellibrachia* species and confirmed range extension for *Lamellibrachia barhami* (Siboglinidae, Annelida) from Costa Rica methane seeps. *Zootaxa* **4504**, 1. doi:10.11646/zootaxa.4504.1.1

McCowin MF, Rowden AA, Rouse GW (2019). A new record of *Lamellibrachia columna* (Siboglinidae, Annelida) from cold seeps off New Zealand, and an assessment of its presence in the western Pacific Ocean. *Marine Biodiversity Records* **12**, 10. doi:10.1186/s41200-019-0169-2

McMullin E, Hourdez S, Schaeffer S, Fisher C (2003). Phylogeny and biogeography of deep sea vestimentiferan tubeworms and their bacterial symbionts. *Symbiosis* **34**, 1–41.

Medina-Silva R, Oliveira RR, Trindade FJ, Borges LGA, Lopes Simão TL, Augustin AH, Valdez FP, Constant MJ, Simundi CL, Eizirik E, Groposo C, Miller DJ, da Silva PR, Viana AR, Ketzer JMM, Giongo A (2018). Microbiota associated with tubes of *Escarpia* sp. from cold seeps in the southwestern Atlantic Ocean constitutes a community distinct from that of surrounding marine sediment and water. *Antonie van Leeuwenhoek* **111**, 533–550. doi:10.1007/s10482-017-0975-7

Miglietta MP, Hourdez S, Cowart DA, Schaeffer SW, Fisher C (2010). Species boundaries of Gulf of Mexico vestimentiferans (Polychaeta, Siboglinidae) inferred from mitochondrial genes. *Deep Sea Research II* **57**, 1916–1925. doi:10.1016/j.dsr2.2010.05.007

Miura T, Kojima S (2006). Two new species of vestimentiferan tubeworm (Polychaeta: Siboglinidae aka Pogonophora) from the Brothers Caldera, Kermadec Arc, South Pacific Ocean. *Species Diversity* **11**, 209–224.

Miura T, Tsukahara J, Hashimoto J (1997). *Lamellibrachia satsuma*, a new species of vestimentiferan worms (Annelida: Pogonophora) from a shallow hydrothermal vent in Kagoshima Bay, Japan. *Proceedings of the Biological Society of Washington* **110**, 447–456.

Nelson K, Fisher C (2000). Absence of cospeciation in deep-sea vestimentiferan tube worms and their bacterial endosymbionts. *Symbiosis* **28**, 1–15.

Nye V, Copley J, Linse K, Plouviez S (2013a). *Iheyaspira bathycodon* new species

(Vetigastropoda: Trochoidea: Turbinidae: Skeneinae) from the Von Damm Vent Field, Mid-Cayman Spreading Centre, Caribbean. *Journal of the Marine Biological Association of the United Kingdom* **93**, 1017–1024. doi:10.1017/S0025315412000823

Nye V, Copley J, Plouviez S (2012). A new species of *Rimicaris* (Crustacea: Decapoda: Caridea: Alvinocarididae) from hydrothermal vent fields on the Mid-Cayman Spreading Centre, Caribbean. *Journal of the Marine Biological Association of the United Kingdom* **92**, 1057–1072. doi:10.1017/S0025315411002001

Nye V, Copley J, Plouviez S, Van Dover CL (2013b). A new species of *Lebbeus* (Crustacea: Decapoda: Caridea: Hippolytidae) from the Von Damm Vent Field, Caribbean Sea. *Journal of the Marine Biological Association of the United Kingdom* **93**, 741–751. doi:10.1017/S0025315412000884

O'Dea A, Lessios HA, Coates AG, Eytan RI, Restrepo-Moreno SA, Cione AL, Collins LS, de Queiroz A, Farris DW, Norris RD, Stallard RF, Woodburne MO, Aguilera O, Aubry M-P, Berggren WA, Budd AF, Cozzuol MA, Coppard SE, Duque-Caro H, Finnegan S, Gasparini GM, Grossman EL, Johnson KG, Keigwin LD, Knowlton N, Leigh EG, Leonard-Pingel JS, Marko PB, Pyenson ND, Rachello-Dolmen PG, Soibelzon E, Soibelzon L, Todd JA, Vermeij GJ, Jackson JBC (2016). Formation of the Isthmus of Panama. *Science Advances* **2**. doi:10.1126/sciadv.1600883

Olu K, Sibuet M, Harmegnies F, Foucher J, Fiala-Medoni A (1996). Spatial distribution of diverse cold seep communities living on various diapiric structures of the southern Barbados prism. *Progress in Oceanography* **38**, 347–376.

Plouviez S, Ball B, Van Dover CL (2017). Population genetics of *Lamellibrachia* sp. 2 deep-sea chemosynthetic tubeworms in the Gulf of Mexico and Caribbean Sea. *unpublished Genbank sequences*.

Plouviez S, Jacobson A, Wu M, Van Dover CL (2015). Characterization of vent fauna at the Mid-Cayman Spreading Center. *Deep Sea Research Part I: Oceanographic Research Papers* **97**, 124–133. doi:10.1016/j.dsr.2014.11.011

Puillandre N, Lambert A, Brouillet S, Achaz G (2012). ABGD, Automatic Barcode Gap

902 Discovery for primary species delimitation. *Molecular Ecology* **21**, 1864–1877.
903 doi:10.1111/j.1365-294X.2011.05239.x
904 Reveillaud J, Reddington E, McDermott J, Algar C, Meyer JL, Sylva S, Seewald J, German
905 CR, Huber JA (2016). Subseafloor microbial communities in hydrogen-rich vent fluids
906 from hydrothermal systems along the Mid-Cayman Rise. *Environmental Microbiology*
907 **18**, 1970–1987. doi:10.1111/1462-2920.13173
908 Ronquist F, Teslenko M, van der Mark P, Ayres DL, Darling A, Höhna S, Larget B, Liu L,
909 Suchard MA, Huelsenbeck JP (2012). MrBayes 3.2: efficient Bayesian phylogenetic
910 inference and model choice across a large model space. *Systematic Biology* **61**, 539–
911 542. doi:10.1093/sysbio/sys029
912 Schneider CA, Rasband WS, Eliceiri KW (2012). NIH Image to ImageJ: 25 years of image
913 analysis. *Nature Methods* **9**, 671–675.
914 Southward EC (1991). Three new species of Pogonophora, including two vestimentiferans,
915 from hydrothermal sites in the Lau Back-arc Basin (Southwest Pacific Ocean). *Journal*
916 *of Natural History* **25**, 859–881.
917 Southward EC, Andersen AC, Hourdez S (2011). *Lamellibrachia anaximandri* n. sp., a new
918 vestimentiferan tubeworm (Annelida) from the Mediterranean, with notes on frenulate
919 tubeworms from the same habitat. *Zoosystema* **33**, 245–279.
920 Southward EC, Schulze A, Gardiner SL (2005). Pogonophora (Annelida): form and function.
921 *Hydrobiologia* **535**, 227–251. Available at:
922 http://www.springerlink.com/index/X2676483HN4U203G.pdf [accessed 12 November
923 2012]
924 Stamatakis A (2014). RAxML version 8: a tool for phylogenetic analysis and post-analysis of
925 large phylogenies. *Bioinformatics* **30**, 1312–1313. doi:10.1093/bioinformatics/btu033
926 Swofford DL (2002). 'PAUP*. Phylogenetic Analysis using Parsimony (*and other Methods)'
927 Version 4. (Sinauer Associates: Sunderland, MA)
928 Thiel V, Hügler M, Blümel M, Baumann HI, Gärtner A, Schmaljohann R, Strauss H, Garbe-
929 Schönberg D, Petersen S, Cowart DA, Fisher CR, Imhoff JF (2012). Widespread

occurrence of two carbon fixation pathways in tubeworm endosymbionts: lessons from hydrothermal vent associated tubeworms from the Mediterranean Sea. *Frontiers in Microbiology* **3**, 423. doi:10.3389/fmicb.2012.00423

Vereshchaka AL, Kulagin DN, Lunina AA (2015). Phylogeny and new classification of hydrothermal vent and seep shrimps of the family Alvinocarididae (Decapoda) Ed A Hejnol. *PLoS ONE* **10**, e0129975. doi:10.1371/journal.pone.0129975

Webb M (1969). *Lamellibrachia barhami*, gen. nov., sp. nov. (Pogonophora), from the Northeast Pacific. *Bulletin of Marine Science* **19**, 18–47.

Williams AB (1998). New marine decapod crustaceans from waters influenced by hydrothermal discharge, brine, and hydrocarbon seepage. *Fishery Bulletin* **86**, 263–287.

Woodside JM, Ivanov MK, Limonov AF (1997). Neotectonics and fluid flow through seafloor sediments in the Eastern Mediterranean and Black Seas. Part 1: Eastern Mediterranean. *Intergovernmental Oceanographic Commission Technical Series* **48**, 1–128.

Woodside JM, Ivanov MK, Limonov AF (1998). Shallow gas and gas hydrates in the Anaximander Mountains region, eastern Mediterranean Sea. *Geological Society, London, Special Publications* **137**, 177–193. doi:10.1144/GSL.SP.1998.137.01.15

Supporting information

Supplementary Tables S1-S8 and Supplementary Figures S1-S3 are provided as separate documents. A DarwinCore file for all specimens deposited is also available as a supplementary file to this manuscript, with data uploaded to the Global Biodiversity Information Facility.

Tables

Table 1. Details of Mid-Cayman Spreading Centre vestimentiferan specimens analysed in this study.

Expedition	ROV dive	Taxon	Latitude (N)	Longitude (W)	Depth (m)	Sample code	Analyses
JC082	ISIS200	*Lamellibrachia* sp. nov.	18.37517	-81.79767	2362	912 (AG25)	Morphology, molecular
JC082	ISIS200	*Lamellibrachia* sp. nov.	18.37517	-81.79767	2362	913 (AG11)	Molecular
JC082	ISIS200	*Lamellibrachia* sp. nov.	18.37530	-81.79773	2363	920 (AG32)	Molecular
JC082	ISIS200	*Lamellibrachia* sp. nov.	18.37530	-81.79773	2363	925 (HW2815)	Molecular
JC082	ISIS200	*Escarpia* sp. nov.	18.37533	-81.79778	2362	915 (AG35)	Morphology, molecular
JC082	ISIS200	*Escarpia* sp. nov.	18.37480	-81.79738	2353	918 (AG22)	Molecular
JC082	ISIS200	*Escarpia* sp. nov.	18.37480	-81.79738	2353	919	Morphology
JC082	ISIS200	*Escarpia* sp. nov.	18.37530	-81.79773	2363	921 (AG23)	Molecular
AT18-16	J2-616	*Lamellibrachia* sp. nov.	18.374691	-81.797349	2376	MCR234	Morphology
AT18-16	J2-616	*Lamellibrachia* sp. nov.	18.374691	-81.797349	2376	MCR498	Morphology
AT18-16	J2-617	*Lamellibrachia* sp. nov.	18.374725	-81.797333	2376	MCR667	Morphology
AT18-16	J2-617	*Lamellibrachia* sp. nov.	18.374725	-81.797333	2376	MCR691	Morphology
AT18-16	J2-612	*Escarpia* sp. nov.	18.374714	-81.797358	2375	MCR010	Morphology
AT18-16	J2-612	*Escarpia* sp. nov.	18.374714	-81.797358	2375	MCR017	Morphology
AT18-16	J2-616	*Escarpia* sp. nov.	18.374691	-81.797349	2376	MCR507	Morphology
AT18-16	J2-621	*Escarpia* sp. nov.	18.374716	-81.797329	2375	MCR1333	Morphology

Table 2. COI uncorrected pairwise p-distances (%) for the genus *Lamellibrachia*. Distances for *Lamellibrachia* sp. 2 are highlighted (herein *L. judigobini* sp. nov.).

		1	2	3	4	5	6	7	8	9	10	11	12	13	14	15	16	17	18	19	20	21
1	*Lamellibrachia satsuma*	-																				
2	*Lamellibrachia juni*	14.9	-																			
3	*Lamellibrachia* sp. L7	14.9	0.0	-																		
4	*Lamellibrachia* sp. L5	15.0	7.0	6.7	-																	
5	*Lamellibrachia* sp. L4	14.8	6.7	6.3	2.6	-																
6	*Lamellibrachia* sp. L6	15.1	6.7	6.5	2.8	1.8	-															
7	*Lamellibrachia barhami*	15.0	7.5	7.2	5.4	5.2	5.3	-														
8	*Lamellibrachia columna*	15.6	7.7	7.4	5.0	4.7	4.8	5.8	-													
9	*Lamellibrachia sagami*	16.1	6.8	6.5	4.3	4.1	4.0	4.9	1.0	-												
10	*Lamellibrachia donwalshi*	16.1	7.2	6.9	4.7	4.4	4.5	5.2	4.7	4.5	-											
11	*Lamellibrachia* sp. 2 GOM	16.8	7.4	7.1	5.2	5.1	5.1	4.7	4.6	4.5	2.5	-										
12	*Lamellibrachia* sp. 2 MCSC (912, AG25)	16.5	7.2	6.8	4.7	4.5	4.5	4.5	4.6	3.8	2.3	0.7	-									
13	*Lamellibrachia* sp. 2 MCSC (920, AG32)	16.5	7.1	6.7	4.5	4.3	4.4	4.4	4.4	3.8	2.2	0.5	0.1	-								
14	*Lamellibrachia* sp. 2 MCSC (913, AG11)	16.4	7.2	6.7	3.9	4.2	4.0	3.9	4.2	3.5	1.9	0.2	0.0	0.0	-							
15	*Lamellibrachia* sp. 2 MCSC (925, HW2815)	16.5	7.0	6.6	4.1	4.1	3.9	4.0	4.3	3.6	2.0	0.2	0.0	0.0	0.0	-						
16	*Lamellibrachia* sp. 2 BAR	16.2	7.3	6.9	4.2	4.2	4.2	4.1	4.5	4.4	2.0	0.2	0.0	0.0	0.0	0.0	-					
17	*Lamellibrachia* sp. 2 T&T	16.2	7.3	6.9	4.2	4.2	4.2	4.1	4.5	4.4	2.0	0.2	0.0	0.0	0.0	0.0	0.0	-				
18	*Lamellibrachia anaximandri*	16.6	7.8	7.6	4.3	5.2	4.7	5.3	5.2	4.6	2.7	2.7	3.2	3.1	2.8	2.7	2.8	2.8	-			
19	*Lamellibrachia luymesi* BH	16.5	7.4	7.1	4.5	4.7	4.6	5.4	4.4	4.0	3.3	2.9	3.0	2.8	2.4	2.4	2.9	2.9	2.3	-		
20	*Lamellibrachia luymesi* GC	16.5	7.4	7.1	4.5	4.7	4.6	5.4	4.4	4.0	3.3	2.9	3.0	2.8	2.4	2.4	2.9	2.9	2.3	0.0	-	
21	*Lamellibrachia* sp. 1	16.5	7.4	7.1	4.5	4.7	4.6	5.4	4.4	4.0	3.3	2.9	3.0	2.8	2.4	2.4	2.9	2.9	2.3	0.0	0.0	-

Table 3. Morphological characters of *L. judigobini* sp. nov. and congeneric species.

	TL, mm	tube collars	TDA, mm	OL, mm	OD, mm	NBL	NSL	NPR	VP, um	TPA, um	TPP, um	VL, mm
L. barhami [1,2,3]	599-724, max 1000-1546	in the anterior tube	7.3-9.0, 8-12	4.5-16	4.5-12	0-25, 19-25	0-4/2-5	n/a	60-150	115-160	n/a	4.5-8
L. columna [4]	700-800, max 820	no, smooth tube	14-20	15-42	8-13	21	08-16	1	65-90	70-120	n/a	8-13
L. juni [5,6]	490-621	in the anterior tube	8.2-12.8 - top, 7.4-11.1 - bottom of a funnel	6.6-12.9	5.2-8.3	22-35	2-3/0-4	n/a	87-99	80-98	n/a	
L.sagami [7]	277.0–661.5 (n=4)	in the anterior tube	9.5–11.2 (n=4)	5.8-22.5 (n=18)	4.4-10.8 (n=18)	19-26 (n=17)	3-6 (n=17)	n/a	59-101 (n=19)	67-130* (n=19)	n/a	3.5-7.3
L. satsuma [8]	60-1000	available	2.5-8.7	1.8-9.8	1-5.6	up to 19	0-4/4-5	n/a	35-63	51-82	n/a	n/a
L. victori [3,9]	up to 240	available	up to 15	13	13	18	7	n/a	n/a	n/a	n/a	13
L. luymesi [5,10, 11, 12]	687	slight collars	3.4-9.7 up to 10	6.6-16	3.4-9.7	15-22	4-8	n/a	55-60	75-85	n/a	x
L. donwalshi [13]	240–265	in the anterior tube	9-10	2.5-9	2-6	10-23	05-11	n/a	33.2-74.7	51.5-83	n/a	3-12
L. anaximandri [3,14, 15]	200+, 800-1530	in the anterior tube (young tubes have larger collars, than adult tubes)	3-9	5.5-17	1.8-6	8-19	3-9	2	55-70	60-95	n/a	2.2-5
***L. judigobini* sp. nov.**	**461-1309 (n=6)**	**in the anterior tube**	**10.8-16.4 (n=6)**	**9-16 (n=5)**	**3.5-9 (n=5)**	**11-23 (n=5)**	**3-6 (n=5)**	**1**	**54-104**	**55-140 (n=5)**	**16-50 (n=4)**	**6-14 (n=5)**

Notes. Superscript references: 1 - (Webb 1969); 2 - (Jones 1985); 3 - (Southward *et al.* 2011); 4 - (Southward 1991); 5 - (Gardiner and Hourdez 2003); 6 - (Miura and Kojima 2006); 7 - (Kobayashi *et al.* 2015); 8 - (Miura *et al.* 1997); 9 - (Mañé-Garzón and Montero 1986); 10 - (van der Land and Nørrevang 1975); 11 - (van der Land and Nørrevang 1977); 12 – (Southward, unpublished data); 13 - (McCowin and Rouse 2018); 14 - (Woodside *et al.* 1997); 15 - (Woodside *et al.* 1998); no superscript - this study. NPR: number of rows of pinnules of the branchial lamellae; NSL: number of the sheath lamellae pairs; OL: obturaculum length; OD: obturaculum width, NBL: number of the branchial lamellae pairs; TL: tube length, TDA: tube anterior diameter, TPA: diameter of the papillae cuticular plaque in the anterior trunk; TPP: diameter of the papillae plaque in the posterior trunk; VD: vestimentum diameter; VL: vestimentum length; VL/OL: the ratio of the length of the vestimentum to the length of the obturaculum; VP: diameter of the papillae plaque in the vestimentum. Red squares: the values are equal to the ones of *L. judigobini* sp. nov. Green squares: the values' range encompasses the range of the values of *L. judigobini* sp. nov.

Table 4. Known and possible distribution localities of *Lamellibrachia* sp. 2 (herein *L. judigobini* sp. nov.).

Region	Locality	Taxon	Mentions	Confirmed
Grenada	Kick'em Jenny	*Lamellibrachia* sp. 2	Amon et al. (2017), Carey et al. (2014, 2015)	unconfirmed
Barbados	unknown	*Lamellibrachia* sp. 2	Plouviez et al. (2017)	molecular
Venezuela	Orenoque	*Lamellibrachia*	Jollivet et al. (1990), Cordes et al. (2007)	unconfirmed
Gulf of Mexico	unknown	*Lamellibrachia* sp. 2	Plouviez et al. (2017)	molecular
Gulf of Mexico	Alaminos Canyon	*Lamellibrachia* sp. 2	Nelson & Fisher (2000), Cordes et al. (2007), Miglietta et al. (2010), Thiel et al. (2012)	molecular
Gulf of Mexico	Atwater Valley	*Lamellibrachia* sp. 2	Cordes et al. (2007), Miglietta et al. (2010)	molecular
Gulf of Mexico	DeSoto Canyon	*Lamellibrachia* sp. 2	Thiel et al. (2012), Cowart et al. (2014)	molecular
Gulf of Mexico	Florida Escarpment	*Lamellibrachia* sp. 2	Cowart et al. (2014)	molecular
Gulf of Mexico	Garden Banks	*Lamellibrachia* sp. 2	Miglietta et al. (2010)	molecular
Gulf of Mexico	Green Canyon	*Lamellibrachia* sp. 2	Cordes et al. (2007), Miglietta et al. (2010), Thiel et al. (2012), Cowart et al. (2014)	molecular
Gulf of Mexico	Mississippi Canyon	*Lamellibrachia* sp. 2	Cowart et al. (2014)	molecular
Gulf of Mexico	Walker Ridge	*Lamellibrachia* sp. 2	Miglietta et al. (2010), Cowart et al. (2014)	molecular
Mid-Cayman Spreading Centre	Von Damm Vent Field	*Lamellibrachia* sp. 2	Jacobson et al. (2013), Plouviez et al. (2015)	molecular
Trinidad and Tobago	El Pilar seeps	*Lamellibrachia* sp. 2	Olu et al. (1996), Amon et al. (2017) Plouviez et al. (2017)	molecular

Table 5. Morphological characters of *E. tritentaculata* sp. nov. and congeneric species.

	TL, mm	TDA, mm	TDP, mm	OL, mm	OD, mm	VL, mm	VD, mm	NL	tentacles kinds	Flattened tentacles	pinnules
E. spicata[1]	63-167+	5.5-9.5	0.5-2	9-13	6.5-11	19.5-34.2	5-9.5	68	external& internal	no	on external tentacles
E. laminata[1]	23-334+	2.9-8	0.5-3	2-10.2	2.2-10.5	6-19.2	2.3-12.9	30-35+	external& internal	no	on external tentacles
E. southwardae[2,3]	300-350, or 600-1900	5-10 (n=64)	2.9-0.2 (n=64)	4.1-13.2 (n=101)	4.2 - 8.8 (n=102)	16.4-42.2 (n=102)	4.3-8.2 (n=101)	13-18	external& internal	external &internal	absent
***E. tritentaculata* sp. nov.**	**192-480**	**4.2-11.5**	**1-2**	**4-11**	**5-10**	**10-16**	**5-10**	**28-43**	**external& internal& intermediate**	**no**	**absent**

Notes. Superscript references: 1 - (Jones 1985); 2 - (Andersen *et al.* 2004); 3 - Ann Andersen, personal communication; no superscript - this study. NL: number of lamellae, OD: obturaculum width, OL: obturaculum length, TDA: tube anterior diameter, TDP: tube posterior diameter, TL: tube length, VD: vestimentum diameter, VL: vestimentum length, VPM: posterior margin of the wings. Red squares: the values are equal to the ones of *E. tritentaculata* sp. nov. Green squares: the values' range encompasses the range of the values of *E. tritentaculata* sp. nov.

Figure captions

Figure 1. Map of the distribution of *Lamellibrachia* and *Escarpia* species (A) and bathymetric map of new species findings at the VDVF (B). (A) Known localities of the species *Lamellibrachia* sp. 2 (described as *L. judigobini* sp. nov. herein) and nearby *Lamellibrachia* species, as well as of the genus *Escarpia* including the MCSC species (described as *E. tritentaculata* sp. nov. herein). (B) Bathymetric map of the VDVF showing sampling locations at 'Marker X18' region and "Vestimentiferan zone".

Figure 2. Results of a Bayesian phylogenetic analysis for a combined dataset (COI, 16S, 18S) for siboglinid vestimentiferans, with posterior probability (%) given at each node, followed by ML bootstrap support values. Missing values indicate clades where the Bayesian and ML analyses differed, while the insert shows *Lamellibrachia* relationships from the best-scoring tree from the ML analysis with bootstrap support values. Locality codes are as follows: MCR, Mid-Cayman Spreading Centre; BAR, Barbados; GOM, Gulf of Mexico; T&T, Trinidad and Tobago.

Figure 3. Haplotype networks for *Lamellibrachia judigobini* sp. nov. COI, *Escarpia tritentaculata* sp. nov. COI, and *Escarpia tritentaculata* sp. nov. HbB2 intron.

Figure 4. *Lamellibrachia judigobini* sp. nov. and *Escarpia tritentaculata* sp. nov. *in situ* at hydrothermal vents of the Mid-Cayman Spreading Centre (A-D) and seeps off Trinidad and Tobago (E-G). (A) *L. judigobini* sp. nov. (pink arrow) and *E. tritentaculata* sp. nov. (yellow arrow) in situ at the Von Damm Vent Field, Mid-Cayman Spreading Centre. Tubes are embedded in rubbly sediment and are aligned roughly parallel to the seabed. (B) A nearby area of similar rubbly sediment with smaller *L. judigobini* sp. nov. and *E. tritentaculata* sp. nov. individuals. Microbial mats, numerous *Iheyaspira bathycodon* gastropods, and some *Lebbeus virentova* shrimps are also visible. (C-D) Detail of two *E. tritentaculata* sp. nov. tubes just

1024 before they enter the rubbly sediment characterising their habitat at the Von Damm Vent
1025 Field. (E) A patch of *L. judigobini* sp. nov. at the El Pilar seep site off Trinidad and Tobago,
1026 alongside live and dead *Bathymodiolus boomerang* mussels, *Alvinocaris* cf. *muricola* shrimp,
1027 and *Kanoia* cf. *meroglypta* gastropods, and other fauna. (F) Cluster of *L. judigobini* sp. nov.
1028 individuals (pink arrow) embedded in carbonate blocks at the El Pilar seep site, larger patches
1029 of *Bathymodiolus childressi* Gustafson, Turner, Lutz & Vrijenhoek, 1998 mussels are also
1030 visible. (G) *L. judigobini* sp. nov. individuals aligned roughly parallel to the seafloor in a more
1031 sedimented region of the El Pilar seep site, with thick microbial mat covering the sediment
1032 and some tube surfaces. Image credit for B-G: Ocean Exploration Trust.
1033
1034 **Figure 5**. Morphology of siboglinid tubes from the Mid-Cayman Spreading Centre (Von
1035 Damm Vent Field). *Lamellibrachia judigobini* sp. nov (A-C) and *Escarpia tritentaculata*
1036 sp.nov. (D-H).
1037
1038 **Figure 6.** Live specimens of (A) *Lamellibrachia judigobini* sp. nov. and (B) *Escarpia*
1039 *tritentaculata* sp. nov. from the Mid-Cayman Spreading Centre, removed from their tubes.
1040 Scales are 10 mm.
1041
1042 **Figure 7.** External view of *Lamellibrachia judigobini* sp.nov. holotype from Mid-Cayman
1043 Spreading Centre. (A, D) – photographs, (B-C) – drawings, anterior end of the worm is up,
1044 papillae are shown only on the certain area, although they cover the whole vestimentum and
1045 trunk. (A, B) ventral view. (C) dorsal view. (D) trunk papillae are positioned in the dense
1046 patches (black arrows) and loose patches (white arrows). bl – branchial lamellae, gcg – genital
1047 ciliated grooves (male) with epidermal folds, OB – obturaculum, ol – obturacular lobe, p –
1048 plumes, sl – sheath lamellae, tp – trunk papillae, TR – trunk, vc – vestimental cavity, vcf –
1049 ventral ciliated field, vnc – ventral nerve cord, vp – vestimental papillae, VT – vestimentum,
1050 vw – vestimental wings.
1051

Figure 8. External morphology of *Lamellibrachia judigobini* sp. nov. from Mid-Cayman Spreading Centre, scanning electron microscopy (SEM). (A-B) Tentacular plume. (A) – overview of the sheath lamellae, (a) - close-up of fused tips; (B) – overview of the branchial lamellae, (b) – close-up of free pinnulated tips. The arrow shows pinnules, the arrowheads show longitudinal rows of cilia, external (hatched) and internal (white) ones. (C) – the anterior end of the dorsal genital ciliated grooves in the vestimentum, male specimen, (D) – the posterior end of the genital groove, male specimen. Arrow shows the groove cavity. (E-K) Different types of the papillae; anterior part is up, except (F) which has an anterior-posterior (a-p) axis indicator, arrows show papillae with openings of the tubiparous glands; arrowheads indicate thickened anterior margins of the plaques of the cuticular plaque papillae. (E) papillae position on the vestimental wing, (F) close-up of the vestimental papillae. (G) Anterior trunk papillae. Picture shows the patch of densely located papillae. (H) Mid trunk papillae. There are loosely located papillae on the non-contracted body wall. (I) Close-up of the trunk papillae. (J) Posterior trunk papillae. (K) Close-up of posterior trunk papillae. cp – cuticular plaque of the papillae, ef – epidermal folds, isw – internal surface of vestimenial wing, lp – lateral pinnules, vnc – ventral nerve cord.

Figure 9. External view of *Escarpia tritentaculata* sp.nov. holotype from Mid-Cayman Spreading Centre and its symbiotic polychaete. A, D – photographs, B, C – drawings of the individuals, anterior end is up, papillae are shown only on the certain area, although they cover the whole vestimentum and trunk. (A, B) dorsal view. (C) ventral view. (D) the obturacular lobes with its symbiotic annelid and (d) Phyllodocidae gen. sp. specimen, dorsal view; arrows show that there were two individuals. epf – external plume filaments, gcg – genital ciliated grooves (male), if – internal plume filaments, ocr – obturacular crust, OB – obturaculum, ol – obturacular lobe, olr – obturacular longitudinal ridge, p – plume, rp – row of the papillae, s – spike half, TR – trunk, tp – trunk papillae, vc – vestimental cavity, vcf – ventral ciliated field, vnc – ventral nerve cord, vp – vestimental papillae, VT – vestimentum, vw – vestimental wings.

Figure 10. SEM of the obturacular structures of *Escarpia tritentaculata* sp.nov. from Mid-Cayman Spreading Centre. (A) Cuticular crust of the obturacular lobes, consisted of two layers: columnar (CL) and horizontal (HL) layers. (B-F) External view of the plume's filaments tips. (B) – the external filaments morphology, (C) – cilia rows of the external filaments. Arrowheads show the longitudinal rows of cilia, external (white) and internal (black) ones. (D) – overview of the internal filaments tips, (d) - close-up of the internal filament tips. Arrows show longitudinal cilia rows at the bases of the filaments' tips. (E) – the longitudinal furrows of the internal filaments. Arrowheads show furrows, which are left after adjoined neighbouring tentacles (white) and furrows left over after rows of cilia which parted off due to the fixation (black arrowheads). (F) The intermediate filaments morphology. Free along the most length as the external ones, and they are thick and bear longitudinal furrows (arrowheads) as the internal ones. Longitudinal furrows are less deep that those of internal filaments. Arrows show longitudinal rows of cilia. cl – columnar layer of the obturacular crust, ft – free tips, fz – fusion zone, hl – horizontal layer of the obturacular crust.

Figure 11. SEM of papillae morphology of *Escarpia tritentaculata* sp. nov. from Mid-Cayman Spreading Centre. Organisation of the vestimental (A-C) and trunk (F) papillae. (A) – overview of the vestimental wing, (a1) – close-up of plaques papillae, (a2) – close-up of the tubiparous gland opening (arrow) next to the plaque papilla (arrowhead). (B) – overview of row of plaques papillae along of the ventral ciliary field, (b) – close-up of plaques papillae. (C) – internal surface of the vestimental wing. Black arrowheads show tubercles looking like non-plaque papillae. (D) – overview of the anterior trunk papillae, (E) – close-up of the anterior trunk papillae. (F) – overview of the posterior trunk papillae arrangement, (f) – conspicuous enlarged tubiparous papillae, the black arrowhead shows gland opening. All arrows show papillae with tubiparous glands openings; white arrowheads show thickened anterior margins of the plaques. Anterior end is up (a1, B, b, E, F, f) or left (A, a2, D, C). cam – vestimental wings

collar anterior margin, cf – ventral ciliary field, cp – cuticular plaque of the papillae, vnc – ventral nerve cord.

Supplementary Figure S1. Tube Results of the Automated Barcode Gap Discovery (ABGD) tool, applied using both (A) Jukes-Cantor and (B) Kimura distances.

Supplementary Figure S2. Tube sizes of *L. judigobini* sp. nov. (A) Length and width parameters of the studied tubes. (B) Trend line of the tube growth.

Supplementary Figure S3. Tube sizes of *E. tritentaculata* sp. nov. (A) Length and width parameters of the studied tubes. (B) Trend line of the tube growth.

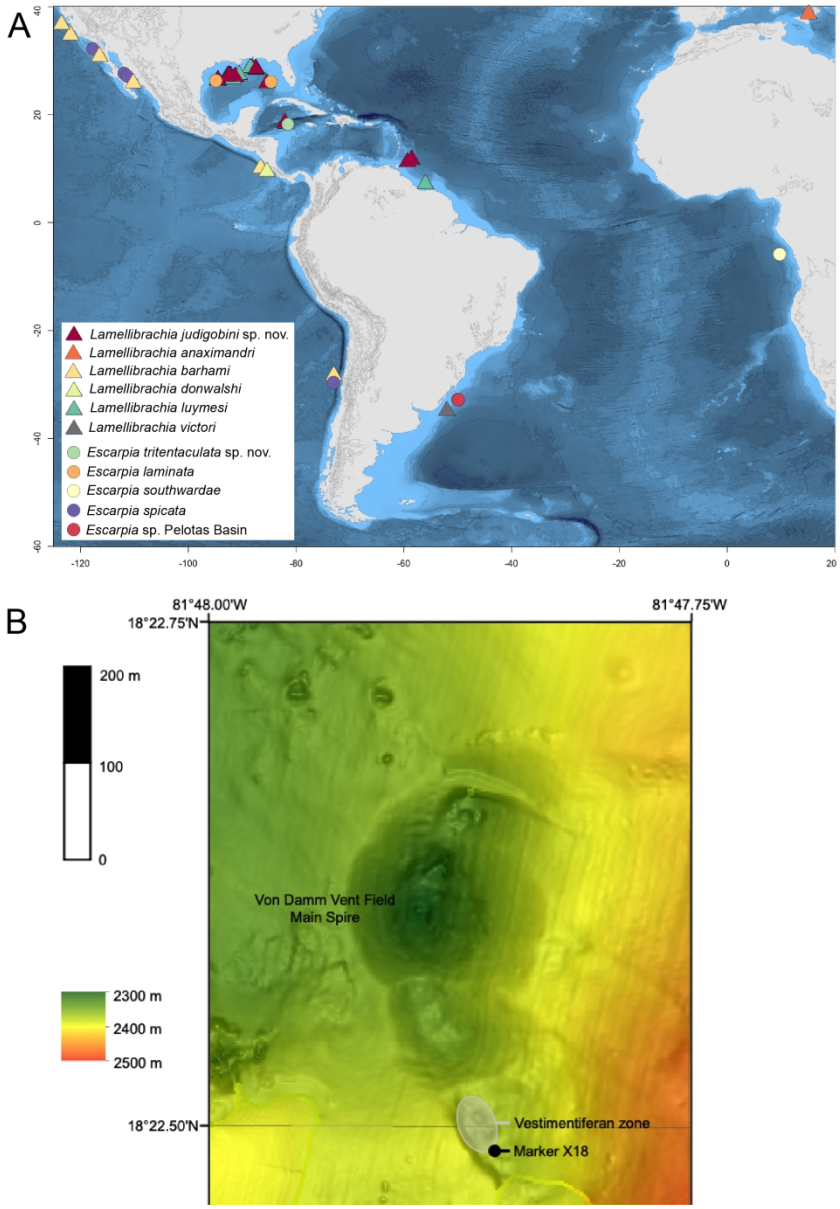

Figure 1. Map of the distribution of *Lamellibrachia* and *Escarpia* species (A) and bathymetric map of new species findings at the VDVF (B).

520x748mm (118 x 118 DPI)

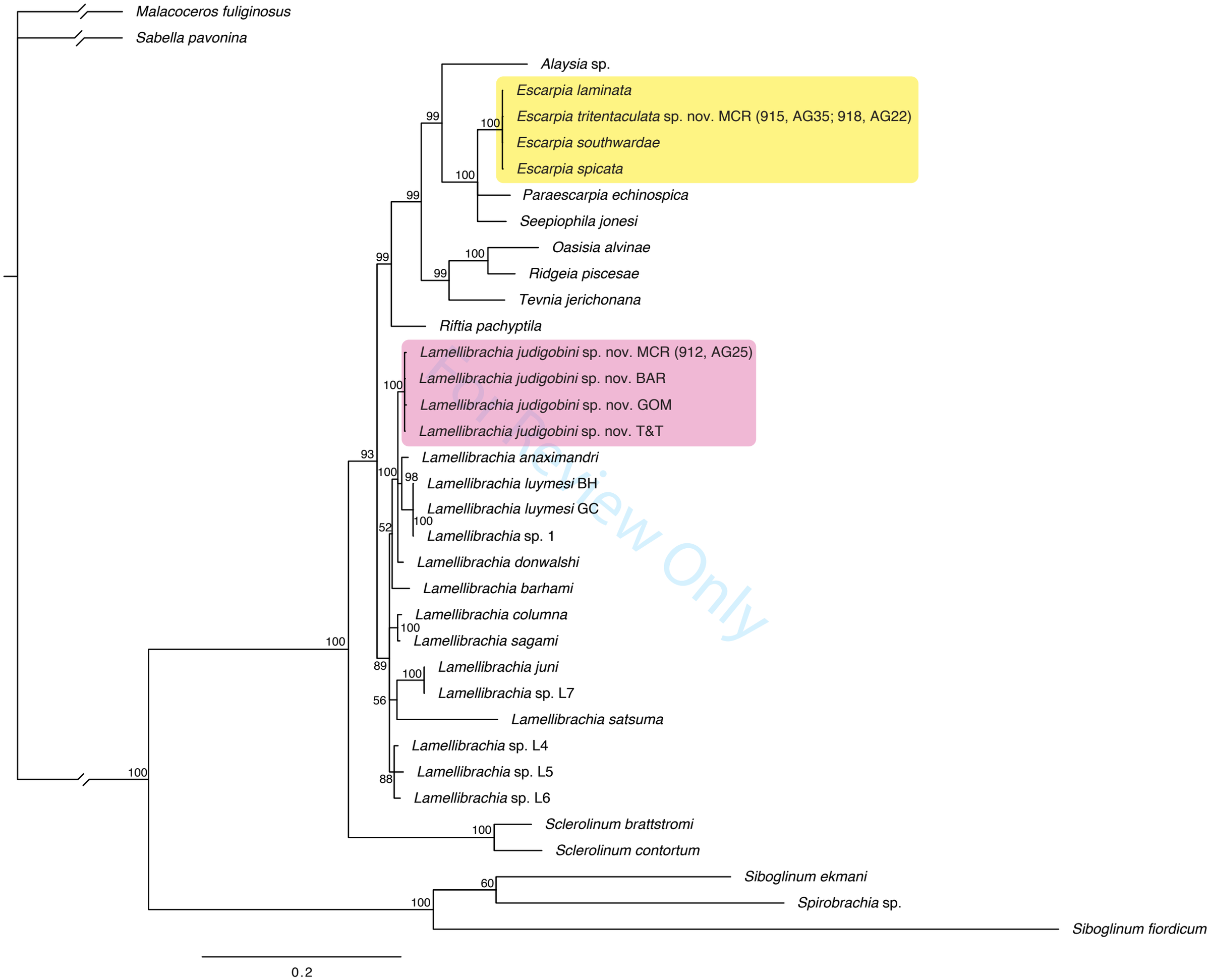

Lamellibrachia judigobini sp. nov.: COI

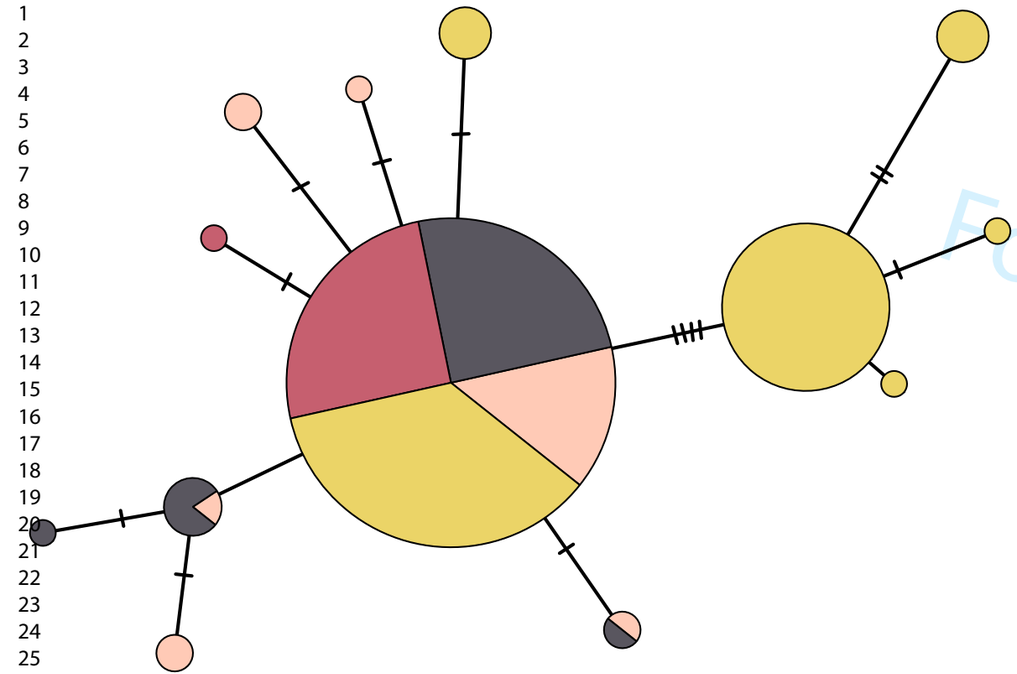

Escarpia tritentaculata sp. nov. : COI

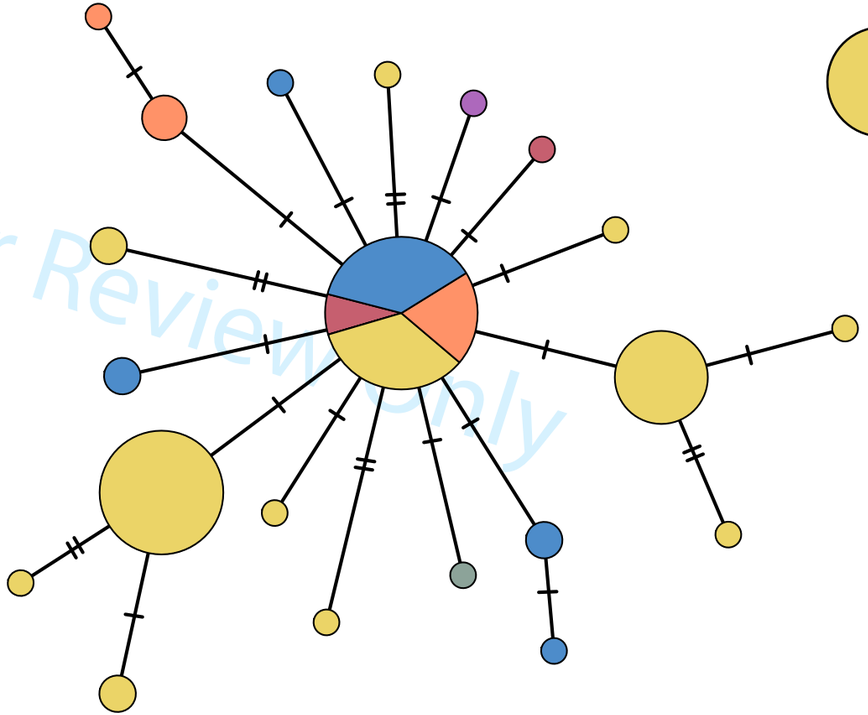

Escarpia tritentaculata sp. nov. : HbB2

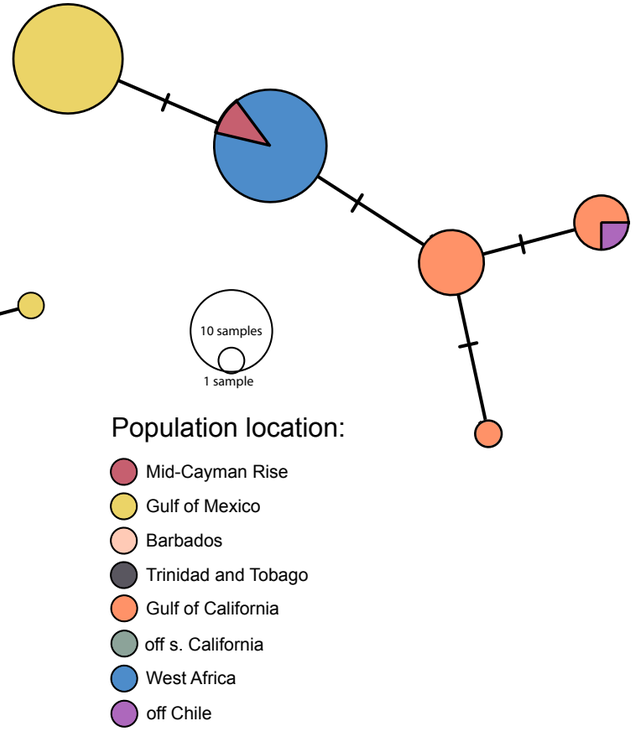

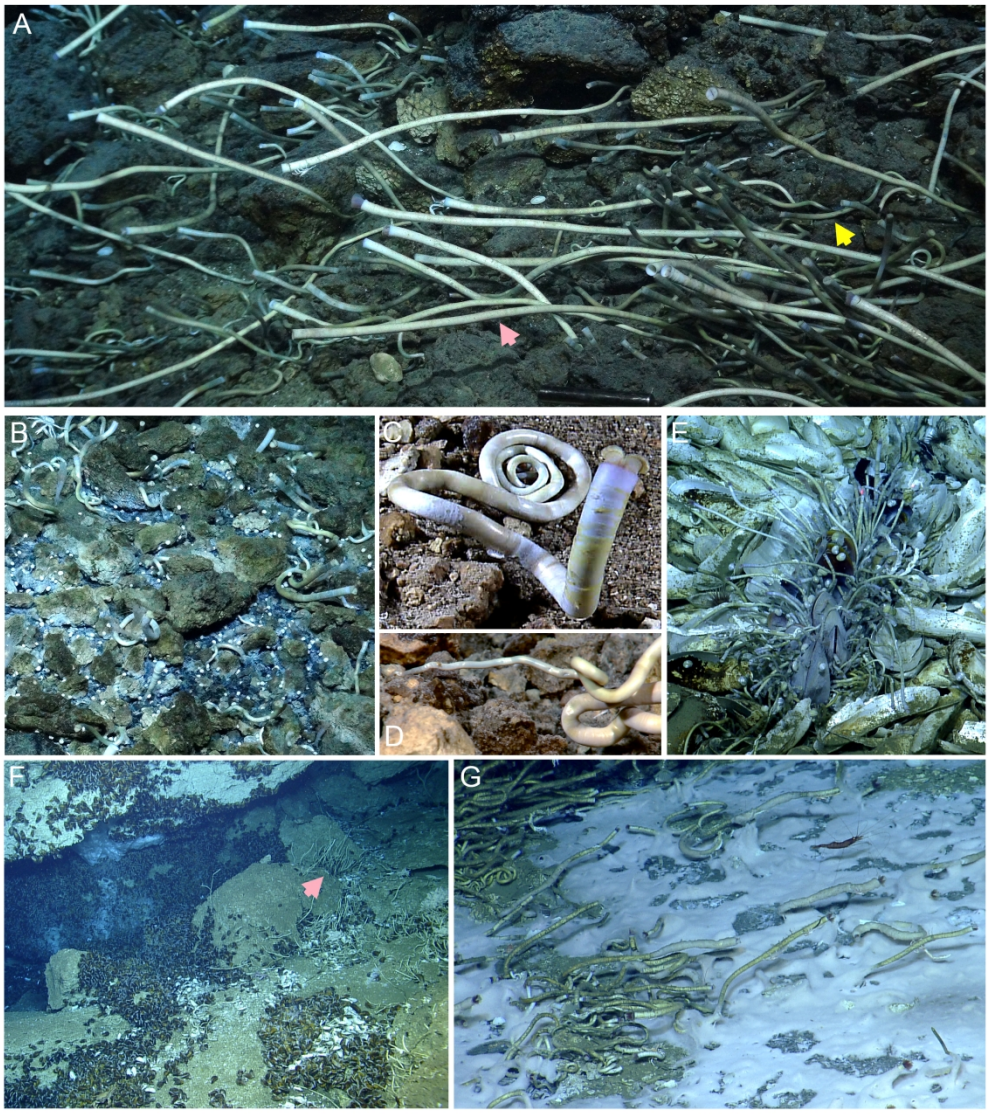

Figure 4. Lamellibrachia judigobini sp. nov. and Escarpia tritentaculata sp. nov. in situ at hydrothermal vents of the Mid-Cayman Spreading Centre (A-D) and seeps off Trinidad and Tobago (E-G).

756x846mm (118 x 118 DPI)

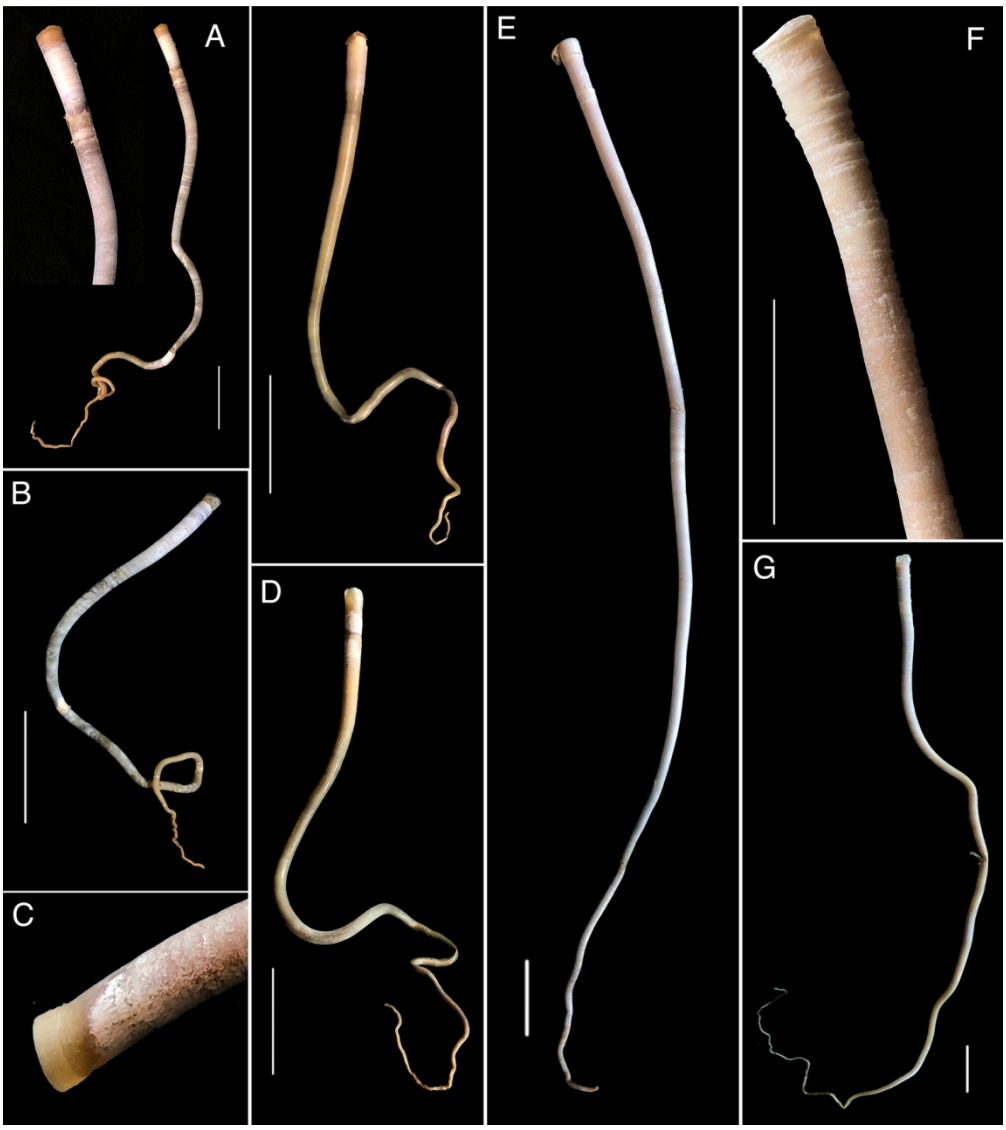

Figure 5. Morphology of siboglinid tubes from the Mid-Cayman Spreading Centre (Von Damm Vent Field).

131x147mm (300 x 300 DPI)

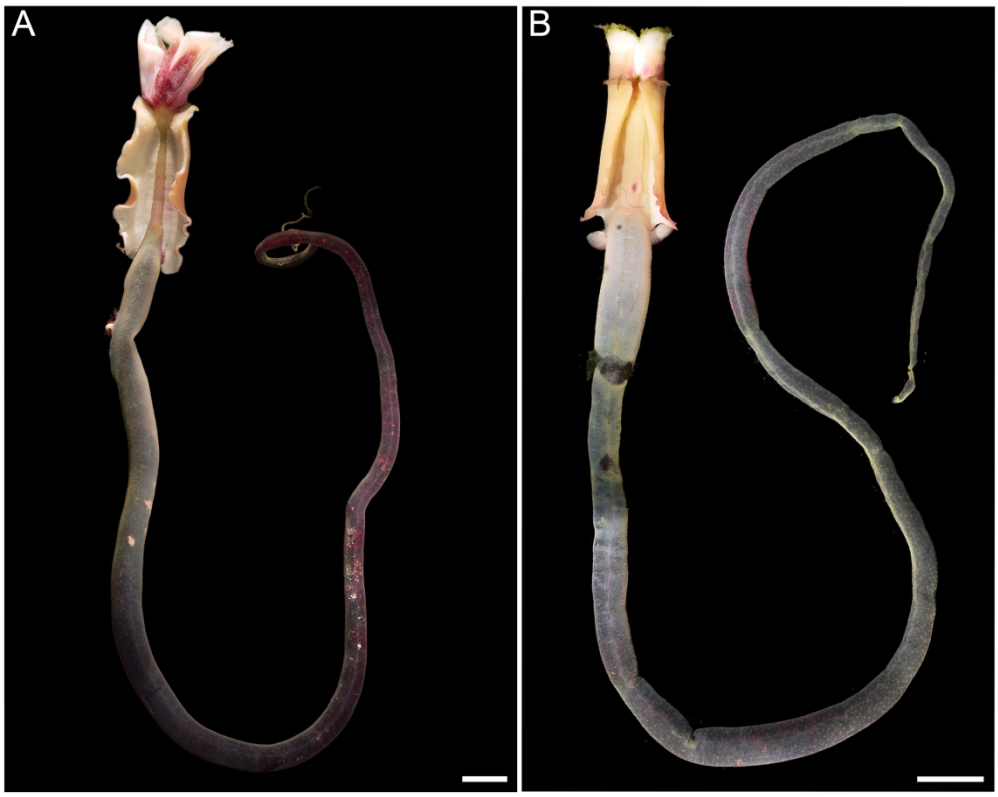

Figure 6. Live specimens of (A) *Lamellibrachia judigobini* sp. nov. and (B) *Escarpia tritentaculata* sp. nov. from the Mid-Cayman Spreading Centre, removed from their tubes.

756x602mm (118 x 118 DPI)

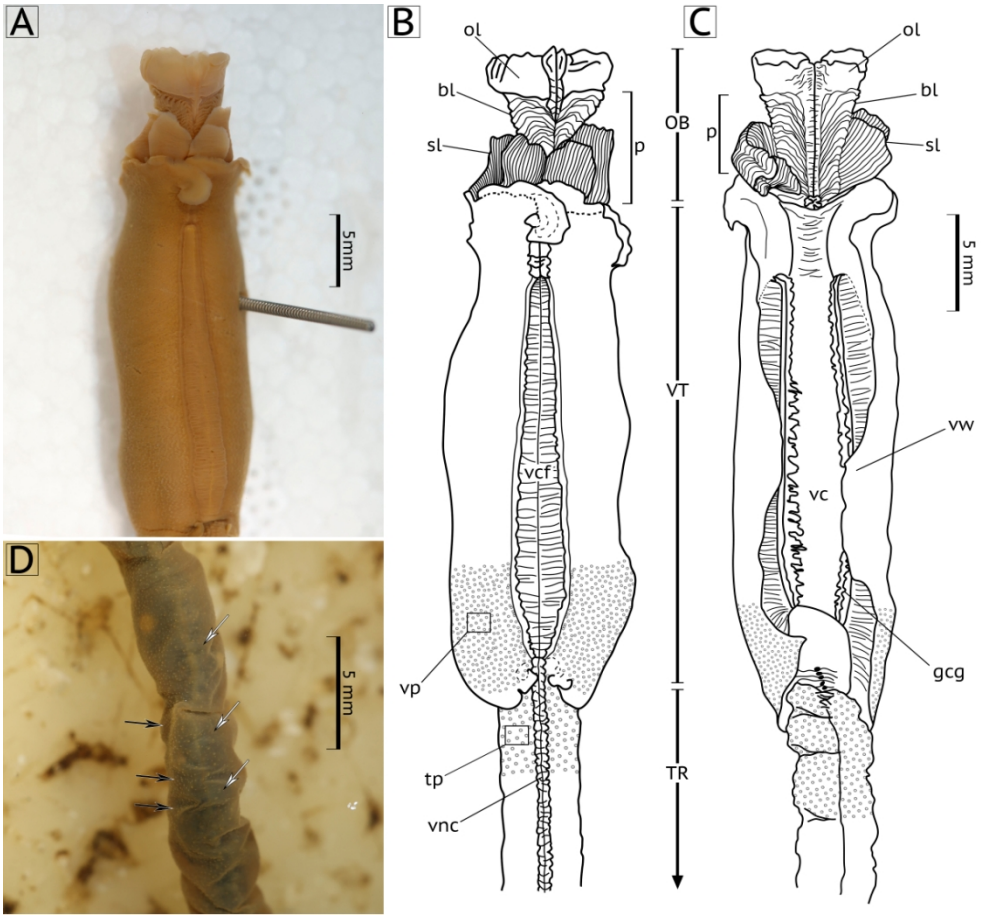

Figure 7. External view of Lamellibrachia judigobini sp.nov. holotype from Mid-Cayman Spreading Centre.

133x121mm (236 x 236 DPI)

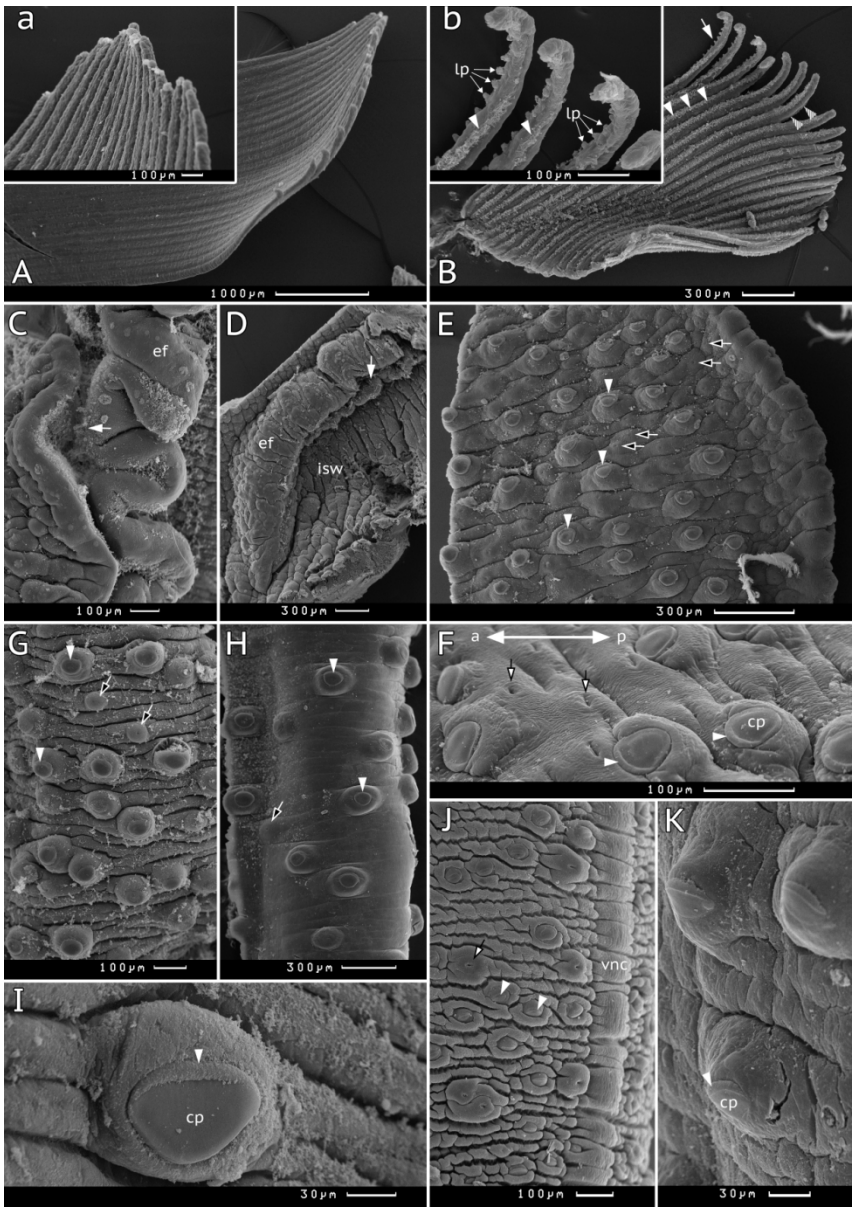

Figure 8. External morphology of Lamellibrachia judigobini sp. nov. from Mid-Cayman Spreading Centre, scanning electron microscopy (SEM).

133x188mm (236 x 236 DPI)

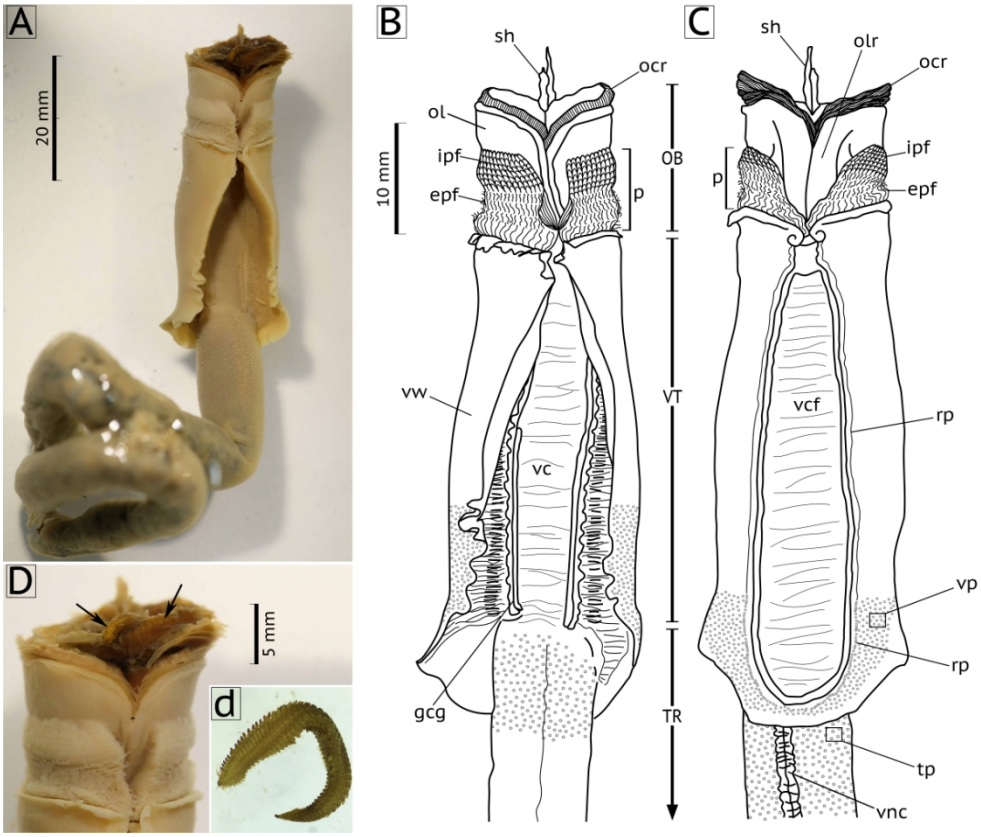

Figure 9. External view of Escarpia tritentaculata sp.nov. holotype from Mid-Cayman Spreading Centre and its symbiotic polychaete.

133x110mm (236 x 236 DPI)

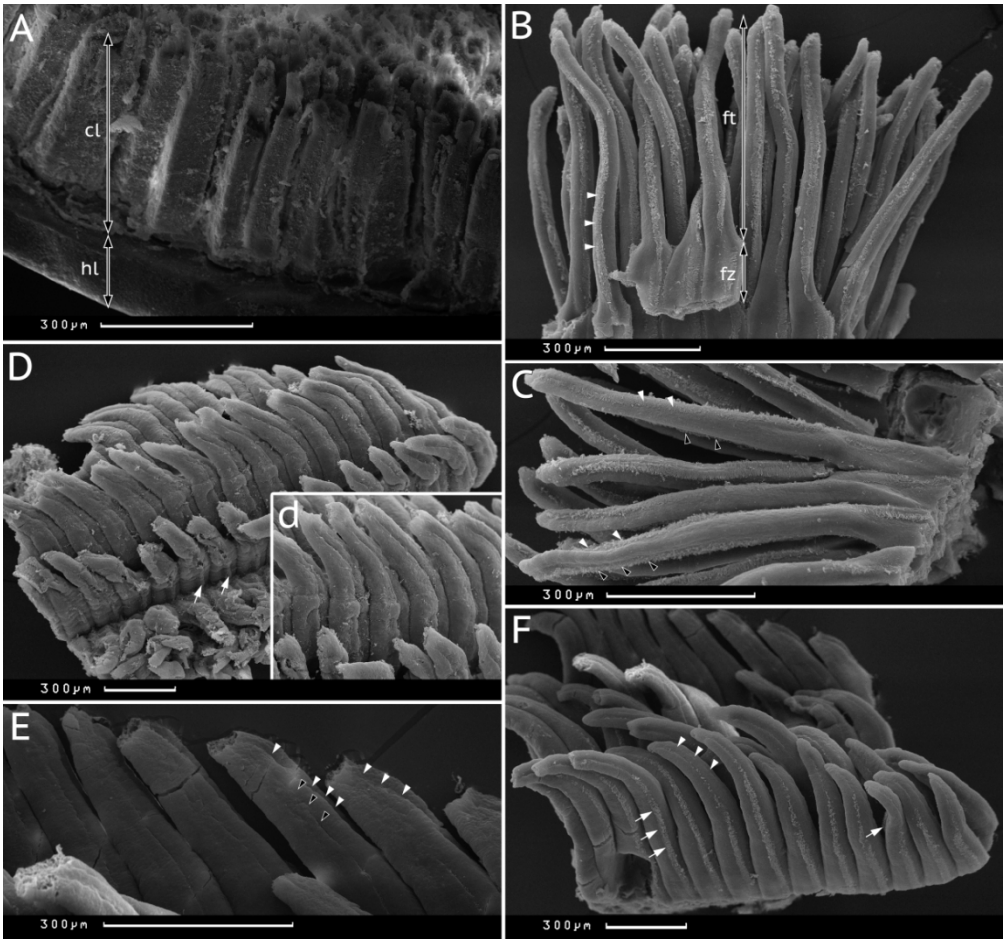

Figure 10. SEM of the obturacular structures of Escarpia tritentaculata sp.nov. from Mid-Cayman Spreading Centre.

133x124mm (236 x 236 DPI)

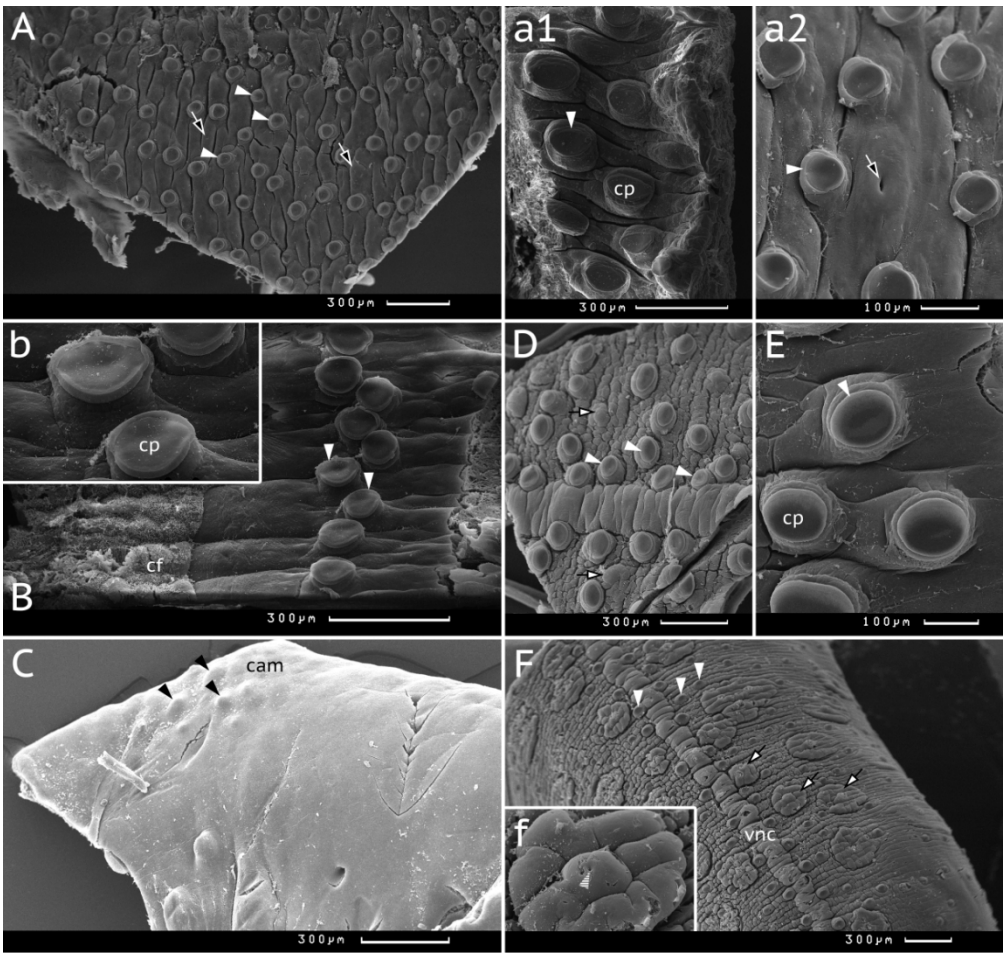

Figure 11. SEM of papillae morphology of Escarpia tritentaculata sp. nov. from Mid-Cayman Spreading Centre.

133x126mm (236 x 236 DPI)